International Journal of Nanomedicine

Dovepress
open access to scientific and medical research

Open Access Full Text Article

REVIEW

Manganese-Based Nanotheranostics for Magnetic Resonance Imaging-Mediated Precise Cancer Management

Ruochen Du[1], Ziwei Zhao[2,*], Jing Cui[3,*], Yanan Li[2]

[1]Department of Laboratory Animal Center, Shanxi Medical University, Taiyuan, Shanxi, 030001, People's Republic of China; [2]College of Medical Imaging, Shanxi Medical University, Taiyuan, Shanxi, 030001, People's Republic of China; [3]College of Public Health, Shanxi Medical University, Taiyuan, Shanxi, 030001, People's Republic of China

*These authors contributed equally to this work

Correspondence: Yanan Li, College of Medical Imaging, Shanxi Medical University, Taiyuan, Shanxi, 030001, People's Republic of China, Email liyanan0213@sxmu.edu.cn

Abstract: Manganese (Mn)-based magnetic resonance imaging (MRI) has become a competitive imaging modality for cancer diagnosis due to its advantages of non-invasiveness, high resolution and excellent biocompatibility. In recent years, a variety of Mn contrast agents based on different material systems have been synthesized, and a series of multi-purpose Mn nanocomposites have also emerged, showing satisfactory relaxation efficiency and MRI performance thus possess the transformation and application value in MRI-synergized cancer diagnosis and treatment. This tutorial review starts from the classification and properties of Mn-based nanomaterials, and then summarizes various preparation and functionalization strategies of nanosized Mn contrast agents, especially focuses on the latest progress of Mn contrast agents in MRI-synergized precise cancer theranostics. In addition, present review also discusses the current clinical transformation obstacles such as unclear molecular mechanisms, potential nanotoxicity, and scale production constraints. This paper provides evidence-based recommendations about the future prospects of multifunctional nanoplatforms, as well as technical guidance and panoramic expectations for the design of clinically meaningful cancer management programs.

Keywords: manganese, magnetic resonance imaging, precise diagnosis, targeted therapy, malignant tumor

Introduction

Cancer remains the major threat to human health with the second leading cause of death after heart diseases, and the burden of cancer increasing dramatically worldwide.[1,2] Early diagnosis and targeted therapy are related to the prognosis and survival of patients. Compared with other diagnostic techniques widely used in clinical practice, magnetic resonance imaging (MRI) has the advantages of non-invasiveness, high spatial resolution, non-ionizing radiation, and soft tissue comparison.[3,4] In addition, MRI provides high-resolution anatomical images for the detection of small tumors and metastases.[5] In brief, the mechanism of MRI is that the hydrogen nucleus in the examined tissue cells resonates under the action of a strong magnetic field. The trajectory of the resonance is recorded by the instrument, and then the data is reconstructed by the computer to form the image for clinical diagnosis.[6] However, MRI without contrast agents lacks broad imaging quality standards leads to local and regional staging impossible, and results in poor differentiation between normal and pathological tissues which affects disease identification.[7,8] Therefore, MRI contrast agents are essential for disease diagnosis.

The most frequently used contrast agents are gadolinium (Gd)- and iron (Fe)-based metal chelates and nanoparticles (NPs).[9] However, the typical shortcomings of the two are gradually revealed: Gd-based contrast agents exhibit relatively fast electronic relaxation, high inherent toxicity, and slow water exchange rates;[10] Fe-based contrast agents exhibit

Received: 19 June 2023
Accepted: 20 September 2023
Published: 26 October 2023

negative imaging defects. Recently, the use of iron chelates and derived nanoprobes as positive contrast agents shows ideal relaxivity in MRI.[11,12] This new research frontier may be a breakthrough direction of Fe-based contrast agents in the future. In contrast, manganese (Mn)-based functional nanomaterials have received much attention in MRI due to their relatively high magnetization spin, fast water particle exchange rate, low side effects, good biocompatibility, crystallinity, and uniformity.[13–16]

Various Mn-derived contrast agents have played a commendable role in illuminating tumors and directing treatment, however, unsatisfactory targeting and specificity have hampered their further development.[17] An ideal diagnostic and therapeutic approach should be specific targeted to the tumor site while minimizing adverse effect to normal tissues.[18] Accordingly, nanotechnology can effectively guide the design and synthesis of various Mn-based contrast agents, improve their performance, and mediate their applications in cancer theranostics.[19] With the development of nanotechnology, Mn-based multifunctional nanocomposites have become safe nanoplatforms for clinical cancer diagnosis, treatment, and monitoring.[20] On the one hand, Mn-based functional nanoplatforms can be expanded by developing novel nanomaterials with high resolution and low toxicity in the future; on the other hand, they are used as carriers to combine with other substances to achieve multi-functionalization, such as MRI-involved multimodal imaging-guided oncotherapy and multimodal synergistic therapy based on biomimetic mineralization strategy.

This review focuses on the Mn-based functional nanoplatforms from the following three aspects: classification of Mn-based contrast agents, preparation methods of various contrast agents, and application of various Mn-based nanotheranostics in MRI-mediated precise diagnosis and targeted treatment of malignancies. Subsequently, some key challenges of nanotoxicity and industrial issues regarding the design of multifunctional nanoagents are discussed. Ultimately, the direction of development and future prospects of Mn-based magnetic nanomaterial-derived cancer nanomedicine are anticipated. These will provide scientific guidance and strategic reference for expanding the construction of Mn nanosystems and their significance in the precise management of cancer.

Classification of MRI Contrast Agents

In recent years, a variety of Mn-based MRI contrast agents, including inorganic and organic contrast agents, have aroused a wide range of basic and clinical research enthusiasm. Inorganic contrast agents include a single Mn metal, Mn oxide, hydroxide, sulfide, Mn ferrite, Mn-based salt, and other material systems. Organic contrast agents are mainly divided into metal-organic small molecule complex and polymer-modified Mn. In this section, representative Mn contrast agents are classified according to the material system. Figure 1 summarized the material types of commonly used Mn-based MRI contrast agents. Table 1 summarized the classification of Mn-based MRI contrast agents.

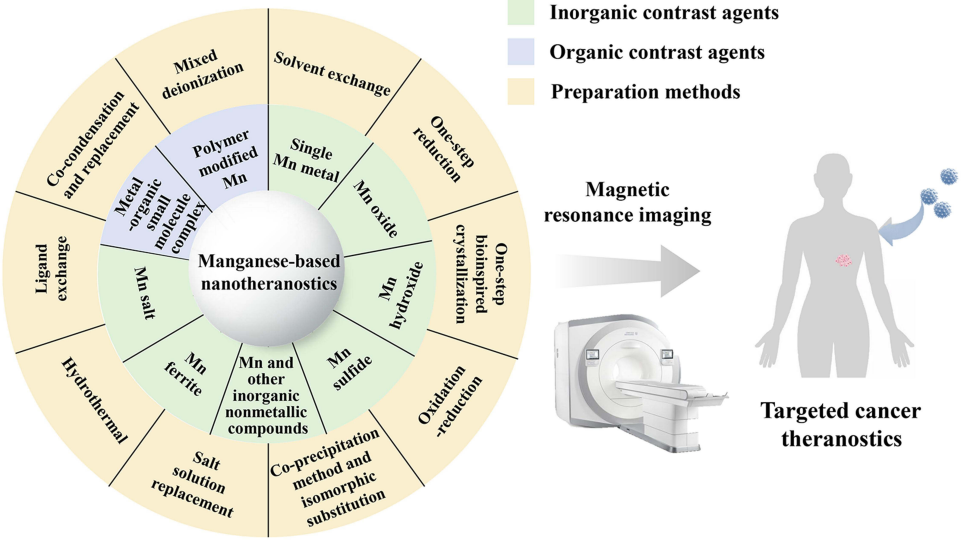

Figure 1 Classification, preparation methods and application of Mn-based MRI contrast agents.

Table 1 Classification of Mn-Based MRI Contrast Agents

Classification		Characteristic	Typical Agents	Ref.
Inorganic	Single Mn metal	Appropriate size, biocompatibility, superparamagnetism, modifiable targeting, photostability	Bispecific antibodies conjugated to Mn NPs	[21]
	Mn oxides	Controllable circulation time, T1-relaxation, water dispersibility, colloidal stability, biocompatibility	MnO MnO_2	[22] [23,24]
	Mn hydroxide	Easily doped with metal ions, high host layer charge density, anion exchange capacity, acid sensitivity, structural tenability, biocompatibility	pH-activated Mn-LDH	[25]
	Mn sulfide	High solubility, no cytotoxicity, photothermal conversion efficiency and stability	Au@MnS@ZnS	[26]
	Mn and other inorganic nonmetallic compounds	Dissociation elasticity, structural stability, internal biosafety, structure-dependent T1 and T2 relaxation	Mn-P nanocomposites	[27]
		Long-term in vivo tracing of tumors	$MnCl_2$	[28]
	Mn ferrite (Mn-Zn)	Biocompatibility, high loading capacity, easily functionalized with silane reagents, saturation magnetization, thermal efficiency, colloidal stability, permeability, low core loss	Mn-doped ferric oxides Mn-Zn ferrite NPs	[29,30]
	Mn salts	Dispersion, colloidal stability, biocompatibility, persistent luminescence, long in vivo circulation, longitudinal relaxation	Mn silicate	[31–34]
		Paramagnetism (room temperature), weak ferromagnetism (low temperature), water dispersion, colloidal stability, high r1 relaxation efficiency	Mn carbonate	[35]
		Porosity, versatility, pH responsiveness, MRI signal amplification, drug release properties	Mn phosphate	[36]
Organic	Metal-organic small molecule complex	Uniform porosity, dispersibility, stability, large specific surface area, inherent properties, strong fluorescence, low toxicity, high T1 relaxation rate	MOFs Mn-quantum dot nanocomplex	[37,38]
	Polymer-modified Mn	Stability, lipotropy, protein affinity, relaxivity	Mn (II)-ethylenediaminetetraacetic acid complex nanocage	[39,40]

Inorganic Contrast Agents

Single Mn Metal

Mn NPs have been widely used in the biomedical field, especially in MRI because of their suitable size, high biocompatibility, superparamagnetism, modifiable targeting, and excellent photostability.[41] For instance, bispecific antibodies were functionalized and conjugated to Mn NPs surfaces to achieve preferential targeting of HER2 receptor and/or epidermal growth factor receptor (EGFR)-expressing tumor cells.[21]

Mn Oxide

Mn oxide NPs, including MnO, MnO_2, Mn_3O_4, MnO_x, and polymetallic oxides, have attracted attention as T_1-weighted MRI contrast agents because of their controllable circulation time of colloidal NPs.[22] Among these NPs, MnO has the advantages of a small volume, simple preparation, and low toxicity. MnO_2 can not only alleviate hypoxia by catalyzing the decomposition of hydrogen peroxide (H_2O_2) into oxygen, but also enhance the T_1-weighted MRI of pH/redox reactions in the tumor microenvironment (TME) and the drug release characteristics after Mn^{2+} decomposition.[23] In addition, considering its good water dispersion, colloidal stability, low toxicity, and responsiveness to TME, MnO_2 has been constructed in various nanoforms,

such as nanodots, nanorods, and nanosheets, to expand its application scope.[24] Other Mn oxide NPs also exhibit excellent physicochemical properties and MRI potential, such as high T_1-relaxation, good water dispersibility, colloidal stability, and biocompatibility.[42]

Mn Hydroxide

Previous studies have reported that layered dihydroxides (LDH) are two-dimensional nanomaterials with extensive medical applications.[43] It has some exciting properties, including easy doping of various metal ions such as Mn^{2+} to prepare functional nanostructures, high host layer charge density and anion exchange capacity, good acid sensitivity due to the protonation of OH groups around the metal ions,[44] good structural tunability and biocompatibility.[45] PH-activated Mn-LDH nanomaterials can accelerate MRI behavior for detecting a variety of cancers.[25]

Mn Sulfide

Au@MnS@ZnS is a novel therapeutic agent with core/shell/shell structure. The inner shell of MnS has a T_1-contrast capability in MRI. MnS NPs obtained by non-covalent modification have high solubility in physiological solutions and no obvious cytotoxicity.[26] In addition, the excellent photothermal conversion efficiency and photothermal stability strengthen the potential of MnS as an MRI contrast agent.[46]

Mn and Other Inorganic Nonmetallic Compounds

This type of material mainly refers to Mn-based nanocomposites with other inorganic nonmetals, such as silicon (Si), carbon (C), phosphorus (P), and halogen. Monodisperse Mn-P nanocomposites with a size of approximately 100 nm exhibit strong Mn dissociation elasticity, structural stability, internal biosafety, and structure-dependent T_1 and T_2 relaxation, which could be used for MRI-guided pharmacokinetic improvement in vivo.[27] As a representative halide, $MnCl_2$ can be used in the long-term tracing of tumors in vivo. In a previous study, $MnCl_2$-labeled cells were found to be highly tumorigenic and could be used to identify early malignant lesions by observing tumor volume development prior to palpation.[28]

Mn Ferrite

Mn ferrite and Mn-doped iron oxide have good biocompatibility and high loading capacity, and can be easily functionalized with various silane reagents.[47] They can not only react with elevated H_2O_2 in cells as a catalyst, to generate O_2 in situ, but also magnetically guide tumors to achieve accurate cancer treatment.[48] It has been proven that Mn-doped ferric oxides show enhanced saturation magnetization and higher thermal efficiency than iron oxide NPs, which has good application prospects in size-dependent MRI and hyperthermia.[29] The synthesized anisotropic Mn-Zn ferrite NPs have an ideal magnetic core lipid shell structure, high colloidal stability, good permeability, and low core loss, which show great potential in MRI-enhanced cancer theranostics by regulating the physical appearance of nanomaterials.[30]

Mn Salt

Mn salts with MRI potential include Mn silicate, carbonate, and phosphate. Among these, Mn silicate has good dispersion, colloidal stability, biocompatibility, persistent luminescence, long in vivo circulation, and high longitudinal relaxation, making it a potential T_1 contrast agent for cancer diagnosis.[31–33]For example, a novel two-dimensional Mn silicate with a high signal-to-noise ratio and degradability has been used in tumor-specific MRI.[34] Mn carbonate NPs exhibit paramagnetism at room temperature and weak ferromagnetism at low temperatures, good water dispersion and colloidal stability, and high r_1 relaxation efficiency, making them excellent contrast agents for T_1 MRI.[35] Mn phosphate NPs have porosity, versatility, strong pH responsiveness, MRI signal amplification, and drug release properties, and can be used for MRI-enhanced cancer therapy in response to acidic tumor environments.[36]

Organic Contrast Agents

Metal-Organic Small Molecule Complex

Represented by metal-organic frameworks (MOFs), metal-organic nanocomplexes have uniform porosity, good dispersibility and stability, large specific surface area, and inherent properties of Lewis acid metals and organic groups, which have been widely used in biomedicine.[37] For example, surface modification of the Mn-quantum dot nanocomplex

showed strong fluorescence, low toxicity, and a high T_1 relaxation rate, which could specifically fluorescently label cancer cells and be used for MRI-enhanced renal cancer diagnosis.[38]

Polymer Modified Mn

As a representative example, the novel Mn (II)-ethylenediaminetetraacetic acid complex nanocage exhibits good stability of the chelate benzothiazole aniline (BTA), high lipotropy BTA derivatives, sufficient protein binding affinity, excellent stability, and relaxivity, which makes it a promising candidate for clinical liver imaging.[39,40] In addition, as a new type of biocompatible material, nanogel loaded with Mn(II) chelates shows high relaxivity values, stability and diagnostic efficiency.[49] Therefore, there is still a lot of room for the development of this type of material by loading various functional nanogels.

The classification of Mn-based MRI contrast agents by inorganic and organic is only one of current forms. In fact, with the increasing number of Mn-based MRI contrast agents being developed, not only to enrich the existing agent system, but also new classifications and sub-classifications will emerge. It should be noted that different material systems often lead to different characteristics, including size, stability, biocompatibility and many other aspects. These characteristics largely determine the application scope or situation of Mn-based MRI contrast agents. Polymer modified Mn may be an attractive research direction. In addition, the combination of these agents with other nanomaterials such as nanogels may result in a more ideal effect.

Preparation Methods of Contrast Agents

The key to preparing good nanomaterials is the control of the technological conditions of these preparation methods, wherein the control of particle size and dispersion is particularly important. The commonly used preparation methods are solvent exchange, one-step reduction, one-step bioinspired crystallization, oxidation-reduction, co-precipitation, isomorphic substitution, salt solution replacement, hydrothermal, ligand exchange, co-condensation and replacement and mixed deionization methods. This is outlined in the following subsections. Table 2 described the synthesis methods of Mn-based NPs and the respective advantages and disadvantages.

Solvent Exchange Method

The solvent exchange method is based on the solubility difference of a solute in different solvents, so that in the solution, a good solvent is introduced with a nonsolvent, and the good solvent is removed to obtain nanoprecipitation. For this method, high temperature is avoided, and it is suitable for preparing thermally unstable or volatile nanomaterials such as Mn oxide NPs. However, this method is expensive and requires a large amount of organic solvent. Residual solvents that are difficult to remove completely are harmful to the human body and can easily cause drug recrystallization and reduce product dispersion. For instance, Savla et al[5] heated a chloroform solution of hydrophobic Mn_3O_4 nuclei, 1.2-distearoyl-sn-glycero-3-phosphoethanolamine-N-[amino (polyethylene glycol) 2000]ammonium salt, and 1.2-distearoyl-sn-glycero-3-phosphoethanolamine-N-[maleimide (polyethylene glycol)2000] ammonium salt to 60°C and then slowly added them to dimethyl sulfoxide. After the evaporation of chloroform, uniform and stable polymer-modified Mn_3O_4 NPs were obtained.

One-Step Reduction Method

The reduction method involves reducing the soluble salt in a solution with a strong reducing agent to obtain nanoprecipitation. This method is commonly used to prepare Mn oxide NPs of several nanometers. It is simple and easy to control; however, the resulting products are not easy to transfer and assemble, and they easily agglomerate and contain impurities. To overcome the clinical application limitations due to the large size of MnO_2 NPs prepared by the multi-step method, Fu et al[24] directly used hydraulic acid oligomer as a reducing agent to reduce sodium permanganate and generate MnO_2 NPs in one step.

One-Step Bioinspired Crystallization Method

The crystallization method involves precipitation of solute crystals by cooling a thermally saturated solution. It can separate highly purified crystals from a solution containing impurities or from a multicomponent molten mixture. This

Table 2 Synthesis Methods of Mn-Based NPs and the Respective Advantages and Disadvantages Description

Method	Advantage	Disadvantage	Typical Agents	Ref.
Solvent exchange method	Avoid high temperature	High cost and a large amount of organic solvents	Mn_3O_4 NPs	[5]
One-step reduction method	Simple and easy to control	The resulting products are not easy to transfer and assemble, and are easy to agglomerate and contain impurities	MnO_2 NPs	[24]
One-step bioinspired crystallization method	Low energy consumption	Growing conditions are difficult to control	MnO_2 NPs	[50]
Oxidation-reduction method	Convenient and reliable	The storage and transportation of products is troublesome	Mn_3O_4 NPs	[42]
Co-precipitation method and isomorphic substitution	The product is single	Uneven stratification of the products	Mn-LDH NPs	[25]
Salt solution replacement method	Traceable gas therapy for tumor pH reactivity	Replacement of the product quality is poor	γ-phase Mn sulfide nanotubes	[51]
Facile hydrothermal method	The obtained product has high purity, good dispersibility, controllable size	Long reaction cycle and highly dependent on production equipment	$FeMn(SiO_4)$ hollow nanospheres	[52]
The ligand exchange method	Simple and novel method	The quantum dots obtained are unstable and tend to coalesce in solution	Water-soluble Mn ferrite NPs	[53]
Co-condensation and replacement reaction	Suitable for the synthesis of metal-organic small molecule complex	Differential isomerization	Hf-based Mn porphyrin nanomaterial	[37]
Mixed deionization	The operation cost of this method is low	The initial equipment investment is large	Mn^{2+}-PDA nanocomposites	[54]

method has a low energy consumption. To simulate the disinfection process of potassium permanganate ($KMnO_4$), Yang et al[50] used a natural biomacromolecule silk fibroin as a reductant and template, and monodispersed MnO_2 NPs were obtained after the redox reaction between $KMnO_4$ and silk fibroin, followed by in situ mineralization.

Oxidation-Reduction Method

The redox method obtains uniform nanostructures by changing the valence state of substances in a solution with an oxidizer or reductant. This procedure is convenient and reliable; however, the storage and transportation of products are troublesome. For example, Foroushani et al[42] stirred a certain amount of a water/ethanol mixture of heated, cooled, purified several times, and centrifuged $KMnO_4$ to obtain uniform Mn_3O_4 NPs.

Co-Precipitation Method and Isomorphic Substitution Method

Co-precipitation is the process by which a precipitant is added to a solution containing multiple cations to precipitate all ions completely. The product obtained by this method is single, but because of the different pH values required for the precipitation of different ions, not all ions can be precipitated simultaneously, resulting in uneven stratification of the products. Mn hydroxide can be prepared via co-precipitation and isomorphic substitution. For instance, Zhang et al[25] prepared a Mg_3Al-LDH suspension by the co-precipitation method and then partially substituted Mg (II) with Mn (II)

ions to obtain Mn-LDH NPs. In the solution of pH 8.5, perfluoropolyether and Mn-LDH NPs self-assembled to form hybrid Mn-LDH@perfluoropolyether nanostructures through electrostatic interactions.

Salt Solution Replacement Method

The salt solution substitution reaction is a chemical process in which an element reacts with a salt solution to form another element and a salt solution. This method is mainly used for preparing Mn sulfide contrast agent. In a typical example, controllable size and biodegradable metastable γ-phase Mn sulfide nanotubes were synthesized using a simple salt solution replacement method for traceable gas therapy-initiated pH-responsive chemodynamic therapy (CDT) of cancer.[51]

Hydrothermal Method

The hydrothermal method is used for preparing Mn salt nanomaterials by heating and pressurizing the reaction system in water, the medium, in a special closed reactor, to form a relatively high-temperature and high-pressure environment, so that the insoluble reactants can be dissolved and recrystallized. The obtained product has high purity, good dispersibility, and controllable size; however, it has a long reaction cycle and is highly dependent on the production equipment. For example, Chen et al[52] ultrasonically mixed an aqueous solution of $FeSO_4.7H_2O$, $MnCl_2.4H_2O$, and NH_4Cl with the water dispersion of silica colloidal spheres, heated mixture to 140°C for 16 h in a Teflon-lined stainless-steel autoclave, to prepare homogeneous and controllable $FeMn(SiO_4)$ hollow nanospheres.

Ligand Exchange Method

The ligand-exchange method generates additional single- or multiple-ligand-protected nanoclusters by exchanging peripheral protective ligands. This is a simple and novel method for preparing hydrophilic Mn ferrite NPs based on superparamagnetic iron oxide NPs. Leal et al[53] prepared water-soluble Mn ferrite NPs smoothly and instantaneously by ligand exchanging with nucleophilic bases, such as triethylamine and gallol-PEG-OH.

Co-Condensation and Replacement Method

Condensation reaction is a process by which two or more organic compounds bond and release smaller molecules to form a new larger molecule. This method is suitable for the synthesis of metal-organic small-molecule complexes. Bao et al[37] directly performed a co-condensation reaction to synthesize an organic tetrakis (4-carboxyphenyl) porphyrin (TCPP) linker and further synthesized a hafnium (Hf)-based Mn porphyrin nanomaterial by inserting Mn into the center through a substitution reaction.

Mixed Deionization Method

The deionization method utilizes an ion exchange function of the ion exchange resin and the selective transmission effect of ion exchange membranes to guide ion directional migration under a direct current electric field to complete the continuous and deep desalination of water. This method can be used to prepare polymer-modified Mn contrast agents, such as PEGylated Mn^{2+}-chelated dopamine NPs. Miao et al[54] added a $MnSO_4{\cdot}H_2O$ solution to a polydopamine (PDA) NPs suspension and reacted mixture to obtain Mn^{2+}-PDA nanocomposites, which were used for MRI-mediated photothermal therapy (PTT) of cancer. The operational cost of this method is low, but the initial equipment investment is large.

Choosing the appropriate preparation method is important for the production of the expected contrast agent. Researchers should first comprehensively consider the characteristics of the target agent and take into account operability and repeatability. In addition, cost control, product purity, safety, and equipment limitations are also factors that cannot be ignored in the selection of preparation methods.

Mn-Based MRI Nanoprobe-Mediated Targeted Cancer Theranostics

Inorganic Mn Contrast Agent-Mediated Cancer Theranostics

Single Mn Metal

Mn metal-based contrast agents have been widely used in cancer theranostics. In a typical example, Sonis et al[55] developed avasopasem Mn by synthesizing small-molecule dismutase mimics, to effectively intervene in severe oral mucositis caused by radiotherapy and chemotherapy in patients with head and neck cancer, which has been confirmed in clinical trials. Cheng et al[56] designed a Mn-deposited iron oxide nanoplatform to trigger an intracellular cascade reaction. The nanosystem effectively induced cell apoptosis accompanied by iron cell droop, and was considered an ideal candidate for the treatment of tumor cytoplasmic iron-binding apoptosis (Figure 2). Zou et al[57] developed a TME-responsive hollow mesoporous Mn-doped silica shell loaded with doxorubicin (DOX), which had ultrasensitive multi-modal diagnostic capability, enhanced anticancer efficacy, and improved biodegradability, thereby improving the comprehensive efficacy. Furthermore, Wu et al[58] prepared mesoporous PDANPs highly loaded with Mn ions. The nanocomposites showed good MRI contrast, high photothermal conversion efficiency, and encouraging antitumor activity in human cervical epithelial carcinoma (HeLa) tumor-bearing mice, making them an ideal choice for MRI-guided photothermal tumor ablation. In an exploratory study, Sishc et al[59] demonstrated that avasopasem Mn increased intracellular H_2O_2 concentration in non-small cell lung cancer and breast adenocarcinoma, and its superoxide scavenging activity had a palliative effect on radiation-induced mucositis in head and neck cancer. This anticancer synergy is currently undergoing phases I to II clinical validation. Furthermore, Yi et al[60] tested the synergistic effect of Mn^{2+} and YM101 in vitro by unidirectional mixed lymphocyte reaction, carboxyfluorescein diacetate succinimidyl ester dilution, and cytokine analysis. Mn^{2+} combined with YM101 synergistically inhibited the growth of multiple cogene mouse tumors and effectively prolonged their survival. A previous study showed that Mn is essential for enhancing the body's innate immune perception and adaptive immune response to tumors. Tumor growth and metastasis were significantly enhanced in Mn-deficient mice and tumor-infiltrating CD^{8+} T cells were sharply reduced.[61] Xiao et al[62] prepared functional nanoplatforms by coating nano selenium onto self-assembled pseudomonas geniculate cell membrane and

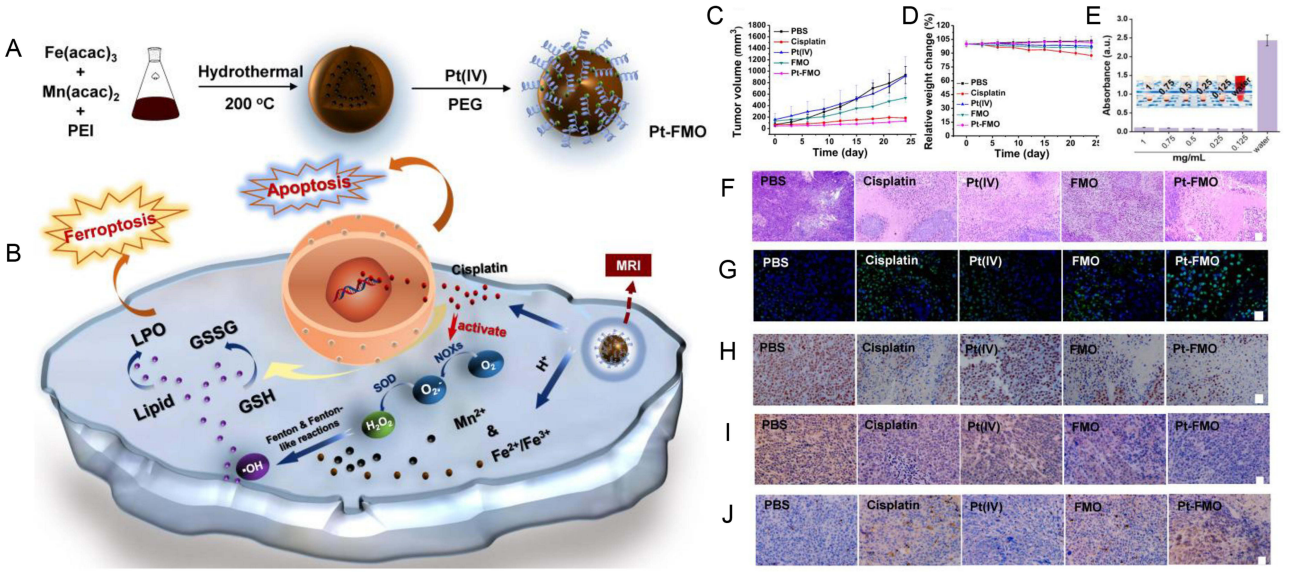

Figure 2 (**A**) Schema of the preparation of magnetic Pt-FMO NPs and its mechanism of inducing apoptosis and ferroptosis for the combined anti-tumor effect. (**B**) The FMO vector sustainably releases Mn^{2+} and Fe^{2+}/Fe^{3+} ions into the acidic environment, which promotes ferroptosis in cells via the Fenton and Fenton-like reactions. Endogenous GSH activates Pt (IV) prodrug and generates cytotoxic cisplatin, thus triggering cellular apoptosis. Meanwhile, cisplatin also mediates conversion of oxygen (O_2) to generate downstream H_2O_2 that further elevates Fenton reactions. (**C**) Tumor volume growth curves. The BALB/c-Nude mice bearing HeLa tumors were treated with various agents. (**D**) Body weight of nude mice. (**E**) Hemolysis assay of Pt-FMO at various concentrations. The UV-vis spectra absorbance of the supernatant of red blood cells at 540 nm incubated with Pt-FMO from 0.125 to 1 mg/mL. (**F-J**) Histological microscopic images. The dissected tumors were stained with H&E (F; scale bar represents 100 μm), Tunel (G; blue fluorescence: Hoechst; green fluorescence: Tunel; scale bar represents 25 μm), Ki67 (H; scale bar represents 25 μm), GPX4 (I; scale bar represents 25 μm) and caspase-3 (J; scale bar represents 25 μm). Reprinted from Cheng J, Zhu Y, Xing X, et al. Manganese-deposited iron oxide promotes tumor-responsive ferroptosis that synergizes the apoptosis of cisplatin. *Theranostics*. 2021;11(11):5418–5429. Copyright 2021.[56]

loading Mn^{2+} ions and DOX, demonstrating the efficacy of mitochondrial and nuclear dual-targeted tumor cell death induction. After modification, Zhu et al[63] developed exosome nanovesicles loaded with a Mn carbonyl group, which showed good performance in tumor targeting, mitochondrial damage, and radiosensitization therapy.

Therefore, Mn metal-based contrast agents have shown excellent anticancer potential in a variety of preclinical animal models and some clinical cases, effectively inhibiting tumor growth and prolonging the survival of patients. For the record, they are pretty cytotoxic. This typical defect limits the application of Mn metal-based contrast agent. However, there is still no effective solution to the cytotoxicity of Mn metal-based contrast agent. At present, most of the biosafety studies of Mn-based nanomaterials rely on in vitro cell viability tests, while a comprehensive in vivo toxicological mechanism analysis of single-Mn metal will undoubtedly enhance the existing understanding.

Mn Oxide

Mn oxide NPs can significantly amplify MRI signals at the tumor site, thus improving the sensitivity of cancer recognition and tumor margin delineation, and enhancing the visibility of metastases. For example, Xu et al[64] constructed a tumor cell membrane coated with bismuth/Mn oxide NPs as a targeted therapy for triple-negative breast cancer. Zhu et al[65] reported a nanotheranostic agent with Mn oxide nanoflowers as the core, PDA as the shell, and indocyanine green (ICG) as the photosensitizer. The release of Mn^{2+} ions made it a TME-sensitive MRI contrast agent for a highly specific diagnosis of liver cancer. Liu et al[66] reported a photoactivated oxygenase hydrogel consisting of Mn oxide and singlet oxygen-reactive preenzyme NPs as a photodynamic therapy (PDT)-mediated combination therapy to effectively inhibit lung metastasis in breast cancer. Furthermore, Tan et al[67] combined oleic acid-modified Mn oxide with temozolomide-obtained nanotherapeutics, showing great potential for MRI-visualized glioma therapy. Wang et al[68] designed cisplatin-loaded mesoporous PDA/MnO_2 NPs mediated by human EGFR2 (HER2)-specific dimers for MRI-enhanced chemotherapy of HER2-positive ovarian cancer. Luo et al[69] constructed nanohybrids composed of superparamagnetic iron oxide, MnO_2, and DOX. The nanoagents acted as inducers for cancer chemotherapy and hyperthermia, and significantly inhibited tumor growth with minimal side effects, demonstrating their great potential as cancer treatments.

In a fascinating report, Zhang et al[70] reported a mesoporous MnO_2 cascade catalytic nanoplatform loaded with acoustic sensitizer and surface-modified with glucose oxidase, which provided attractive opportunities as cancer therapy. Furthermore, pH-sensitive MnO_2@bovine serum albumin (BSA) NPs showed MR contrast signal amplification stimulated by the acidic extracellular environment of solid tumors.[71] Hu et al[72] chemically synthesized a drug delivery vector, PEG coated hollow MnO_2, which significantly inhibited the proliferation of endometrial cancer. In other cases of clinical synergy, Hou et al[73] synthesized a biocompatible MnO_2-containing agarose hydrogel using the sol-gel method for an enhanced PTT/PDT combination. Shen et al[74] self-assembled the ICG derivative CyI and chitosan to form nanosized MnO_2 through electrostatic interaction and Mn-N coordination, effectively alleviating hypoxia in the TME. Another PEG-MnO_2-osteopontin siRNA nanocomplex was constructed using a modular streptavidin bridge, which effectively inhibited the progression of renal cancer in vitro and in vivo in 786-O tumor-bearing mice.[75] Furthermore, Nie et al[76] designed MOF-coated MnO_2 nanosheets that strongly inhibited survivin after loading DNAzyme (DZ) and DOX, thus achieving a chemotherapy cogene therapy for cancer (Figure 3). Wang et al[77] constructed a glutathione (GSH)-triggered Au@MnO_2 nanoplatform for photoacoustic/MRI dual-enhanced synergistic photothermal cancer chemotherapy. Fan et al[78] used surface-grown MnO_2 to assist in the synthesis of Fe_3O_4 NPs and realized near-infrared fluorescence/photoacoustic imaging-monitored synergistic anticancer efficiency. Jain et al[79] synthesized Mn oxide nanocubes by a chemical precipitation method and modified their surfaces with serotonin-stearic acid biocoupling to achieve liver cancer targeting. Through an ingenious design, Ding et al[80] coated chromium-doped zinc gallate NPs with Mn^{3+} oxides. Through a fenton-like reaction, endogenous H_2O_2 was transformed into highly toxic hydroxyl radicals, which could accurately diagnose deep tumors and effectively inhibit tumor growth without external activation energy.

It is worth noting that new nanomaterials based on MnO_2 have been widely developed in recent years. These materials are often multifunctional. For example, Guan et al[81] provided a biodegradable mesoporous zeolitic-imidazolate-framework@MnO_2/doxorubicin hydrochloride nanocomposites to achieve enhanced sonodynamic therapy/CDT/chemotherapy by promoting oxidative stress and overcoming the multidrug resistance, and Liu et al[82] constructed an ultrathin-FeOOH-coated MnO_2 nanospheres as sonosensitizers to achieve effective anti-tumor efficacy by simultaneously increasing the yield of reactive oxygen species and

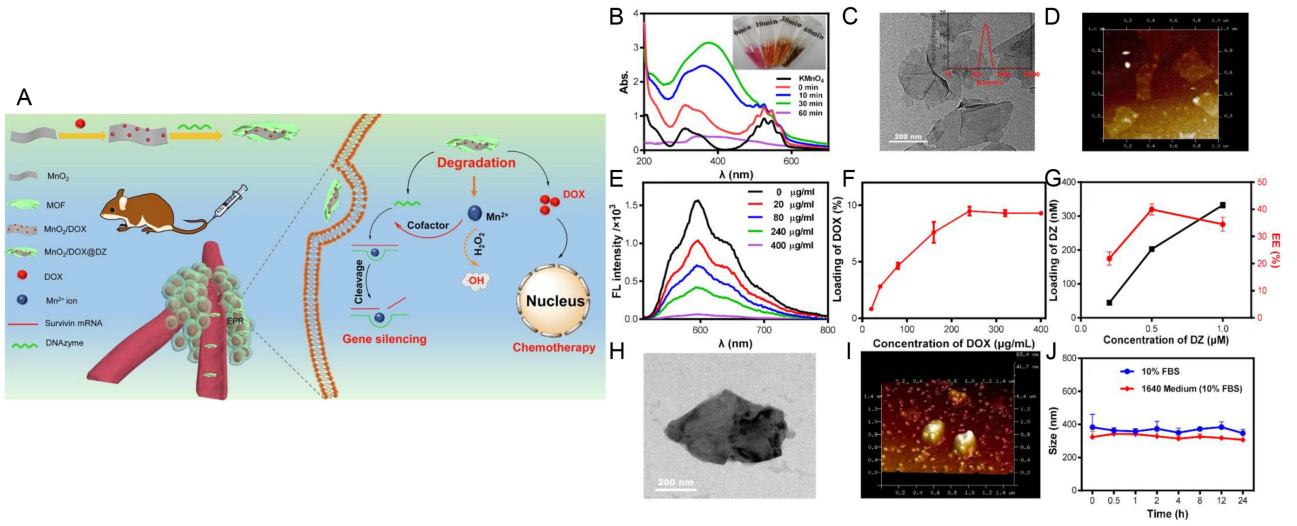

Figure 3 (**A**)The schematic illustration the construction of MnO_2/DOX@DZ and its synergistic antitumor mechanism. Upon endocytosis, the MnO_2/DOX@DZ is degraded by intracellular GSH and acidic environment to release DOX and DZ, and the produced Mn^{2+} exerts excellent Fenton-like activity to generate highly reactive •OH. In addition, Mn^{2+} could also act as metal cofactor to activate DZ to silence survivin expression, resulting in synergistic antitumor with DOX. (**B**) UV-vis spectra monitoring the reaction over a time-course from 0 to 60 min. Inset: The appearance of each tube with different reaction time. (**C**) transmission electron microscopy (TEM) and dynamic size of MnO_2 nanosheets. (**D**) The atomic force microscopy (AFM) of MnO_2 nanosheets. (**E**) The fluorescence of DOX after adding different concentrations of MnO_2 nanosheet. (**F**) The loading capacity of DOX on MnO_2 as a function of DOX concentration. (**G**) The loading capacity and loading efficiency of DZ as a function of DZ concentration. (**H**) The TEM and (**I**) AFM microscopic images of MnO_2/DOX@DZ. (**J**) The stability of MnO_2/DOX@DZ under different conditions. Reprinted from *Int J Pharm,* 585, Nie Y, Li D, Peng Y, et al. Metal organic framework coated MnO(2) nanosheets delivering doxorubicin and self-activated DNAzyme for chemo-gene combinatorial treatment of cancer. Reprinted from *Int J Pharm*, 585, Nie Y, Li D, Peng Y, et al. Metal organic framework coated MnO(2) nanosheets delivering doxorubicin and self-activated DNAzyme for chemo-gene combinatorial treatment of cancer. 119513, Copyright 2020, with permission from Elsevier.[76]

tuning TME. There are also some nanomaterials that show the effect of tumor immunotherapy, such as TME responsive MnO_2-melittin nanoparticles and MnO_2 nanoparticles with high anti programmed death ligand 1 encapsulation efficiency, which synthesized by Tang et al[83] and Deng et al[84] respectively. Another interesting discovery is about the diabetic patients after tumor surgical resection. Specifically, a degradable self-enhanced cascade catalysts CS/MnO_2-GOx nanocatalysts proposed by Wang et al[85] for antitumor/antibacterial therapy and promotion of wound healing.

In short, although the synthesis and therapeutic potential of various Mn oxides are different, existing reports have clearly demonstrated that TME-sensitive active targeting NPs can preferentially concentrate at the tumor sites, thereby improving the sensitivity of MRI and anticancer efficacy. As a controllable drug delivery system, Mn oxide-derived tumor-targeting nanomaterials have a wide therapeutic window, low toxicity, good biocompatibility, strong adsorption capacity, and excellent therapeutic effects. In addition, the inherent pH sensitivity of Mn oxides has prompted scientists to devote considerable effort to explore their novel clinical potential as an intelligent cancer treatment in the future. Table 3 described the applications of Mn oxide-based nanomaterials in cancer diagnosis and treatment.

Mn Hydroxide

In recent years, multifunctional NPs based on Mn hydroxide have been widely used for effective detection and treatment of cancer. Zuo et al[45] prepared dual-functionalized layered Mn dihydroxide NPs, which proved to be an effective anticancer drug/gene delivery system for T_1-weighted MRI-guided brain cancer treatment. Xie et al[86] prepared Mn-doped layered NaOH NPs through a simple two-step synthesis method and demonstrated excellent photothermal properties and T_1-weighted MRI capability, thus providing a potentially effective platform for biodegradable inorganic nanotherapy. Enlightened by this, Wen et al[87] self-assembled layered coal seam dihydroxy compounds and MnO_2 to prepare a multifunctional nanocervator as a selective combination cancer therapy. After co-loading hydrophilic DOX and hydrophobic paclitaxel (PTX), the nanosystem showed an effective combination of chemotherapy against liver cancer. Liao et al[88] synthesized a Mn hydroxide nanocapsule with a high loading capacity and strong catalytic activity, which could effectively relieve hypoxia in tumor tissues and improve the synergistic anticancer effect. Yan et al[89] synthesized CoMn-LDH nanosheets using a bottom-up approach and surface modification with photosensitizer chloride e6 (Ce6). The nanosystem showed satisfactory anticancer activity and promoted the complete apoptosis of cancer cells to remove tumors.

Table 3 Applications of Mn Oxide-Based Nanomaterials in Cancer Diagnosis and Treatment

Nanoagent	Synthesis Method	Shape	Size (nm)	Therapeutic Mode	Tumor	Ref.
Bismuth/Mn oxide NPs	Reverse-microemulsion method	Honeycomb-like structure	81.9 ± 1.6	PTT PDT	4T1 mouse breast cancer cells	[64]
Mn oxide, PDA	Fast aqueous phase synthesis method	Amorphous structure	100	PTT PDT	LM3, HepG2, SNU-387 human liver cancer cells	[65]
Mn oxide and singlet oxygen-reactive preenzyme NPs	Mimick the disinfection process of $KMnO_4$	A loose structure	40	PDT	4T1 mouse breast cancer cells	[66]
iRPPA@TMZ/MnO	Sonification	Micellar	71 ± 15	Chemotherapy	C6 mouse glioma cells	[67]
Mesoporous PDA/ MnO_2/ PDA NPs	A Nano-emulsion assembly approach	Mesostructured morphologies	119	Chemo-radiotherapy	SKOV-3 HER2 human positive ovarian tumor cells	[68]
IO@MnO_2@DOX	Mild Ultrasonication method	Crystal	221.93 ± 19.36	Magnetic hyperthermia and chemotherapy	4T1 mouse breast cancer cells	[69]
H-MnO_2-PEG	Chemical synthesis	Spherical	150	Chemotherapy	RL95-2 human endometrial cancer cells	[72]
Agarose@SH/ MnO_2/ Ce6	A sol gel process	Loose structure	110	PTT PDT	4T1 mouse breast cancer cells	[73]
PEG-MnO_2-OPN	Oxidation	A typical two-dimensional morphology	195	Chemophoto-thermal therapy PTT	786-O human renal cancer cells	[75]
MnO_2/DOX@DZ	Centrifugation	2D sheet-like morphology	230	Chemotherapy CDT	A549 human lung adenocarcinoma cells and MDA-MB-231 human breast cancer cells	[76]
Au@MnO_2	Reduction method	Core-shell structure	Core size of ~25 nm/shell thickness of ~14 nm	Photothermal-enhanced CDT	4T1 mouse breast cancer cells	[77]
Fe_3O_4@MnO_2 CSL/Ce6	Coprecipitation method	Irregular morphology	100	Chemotherapy PDT	Bel-7402 human liver cancer cells	[78]
DOX-ST-SA@MNCs	Chemical precipitation method	Uniform and cuboid shape	21	PTT Hyperthermia therapy	HepG2 human liver cancer cells	[79]
Mn-ZGGOs	Sonication	Uniform	20	PDT	U-87MG human brain astroglioblastoma cells	[80]
mZMD	Redox method	Polygonal shape and porous structure	230	Sonodynamic therapy CDT chemotherapy	HeLa human cervical cancer cells	[81]
MnO_2@FeOOH	Comproportionation reaction and replacement reaction	Spherical	200-400	Sonodynamic therapy	MDA-MB-231 human breast cancer cells	[82]

(*Continued*)

Table 3 (Continued).

Nanoagent	Synthesis Method	Shape	Size (nm)	Therapeutic Mode	Tumor	Ref.
MnO_2-melittin	Coprecipitation method	Spherical	~ 58	Immunotherapy	B16 mouse melanoma cells MC38 mouse colorectal cancer cells MB49 mouse bladder cancer cells	[83]
αPDL1@MnO_2	Biomimetic mineralization method	Spherical	100	Radio-immunotherapy	T26 mouse colorectal cancer cells	[84]
CS/MnO_2-GOx	Redox reaction	Spherical	~ 182	Starvation therapy CDT	A375 human melanoma cells	[85]

Abbreviations: IRPPA, polyethylene glycol-poly(2-(diisopropylamino)ethyl methacrylate-based polymeric micelle containing internalizing arginine-glycine-aspartic acid; TMZ, temozolomide; IO, iron oxide; SH, sodium humate; OPN, osteopontin; CSL, celastrol; ST-SA, serotonin-stearic; ZGGO, zinc gallogermanate; mZMD, mesoporous zeolitic-imidazolate framework@MnO_2/doxorubicin hydrochloride; αPDL1, anti-programmed death ligand 1; CS, chitosan; GOx, glucose oxidase; Ref, reference.

In brief, Mn hydroxide nanomaterials are simple to synthesize, biocompatible, and sensitive to TME. Meanwhile, they enhance T_1/T_2 relaxation and improve MRI accuracy, showing great potential for biomedical applications. However, these nanomaterials still mainly in the research stage, and their advantages and potentialities have not been fully transformed in clinical practice. How to systematically obtain a large amount of reliable biosafety-related data is also a major challenge for Mn hydroxide nanomaterials.

Mn Sulfide

Conventional radiotherapy has been widely used in the clinical treatment of cancer. The effect of MnS contrast agents combined with radiotherapy is remarkable. Li et al[26] synthesized PEG-functionalized Au@MnS@ZnS core/shell/shell NPs. The NPs effectively accumulated and were retained at the tumor site after intravenous injection, showing T_1-weighted MRI-guided significant inhibition of tumor growth. Chen et al[46] designed CuS-MnS_2 nanoflowers as promising nanotheranostic agents for the combined PTT/PDT of ovarian cancer. He et al[51] synthesized metastable γ-phase MnS nanotubes with controllable sizes and biodegradability using a simple wet chemical method and protected them with BSA. After intravenous injection, MnS@BSA exhibited T_1-weighted MRI-activated tumor growth inhibition and significantly prolonged the lifetime of the tumor-bearing mice (Figure 4). Ke et al[90] synthesized two-dimensional Cu_2MnS_2 nanoplates using a simple and environmentally friendly process for MRI/multispectral photoacoustic tomography dual-mode imaging-guided PTT for cancer in the NIR-II window. Further introducing the radiosensitizer, a novel nanoprobe was developed and its application prospects in imaging-enhanced radiotherapy for cancer were explored.

Due to the positive effect of Mn sulfide contrast agent in conventional radiotherapy, the combination of the two should be given priority in future clinical treatment. At the same time, researchers are inspired to develop targeted treatment programs based on the characteristics of different nanomaterials, which firstly depends on the further enrichment and development of Mn-based functional nanoplatforms.

Mn and Other Inorganic Nonmetallic Compounds

Contrast-enhanced MRI based on Mn and inorganic non-metallic composites is essential for the diagnosis and monitoring of cancer. For instance, Irmania et al[91] synthesized Mn-doped Cquantum dots via a one-pot hydrothermal method using waste green tea as the raw material. By coupling the terminal amino groups with folic acid and Ce6, it specifically targeted folate receptor-overexpressing HeLa cells and exerted a magnetic fluorescence PDT effect. Atif et al[92] prepared Mn-doped cerium oxide nanocomposites by a hydrothermal method, which exhibited considerable cytotoxicity and was considered as a promising candidate for the targeted therapy breast cancer. Sha et al[93] constructed a multifunctional nanoplatform by in situ doping of Mn in gold-core mesoporous silica NPs and loading DOX to specifically target and

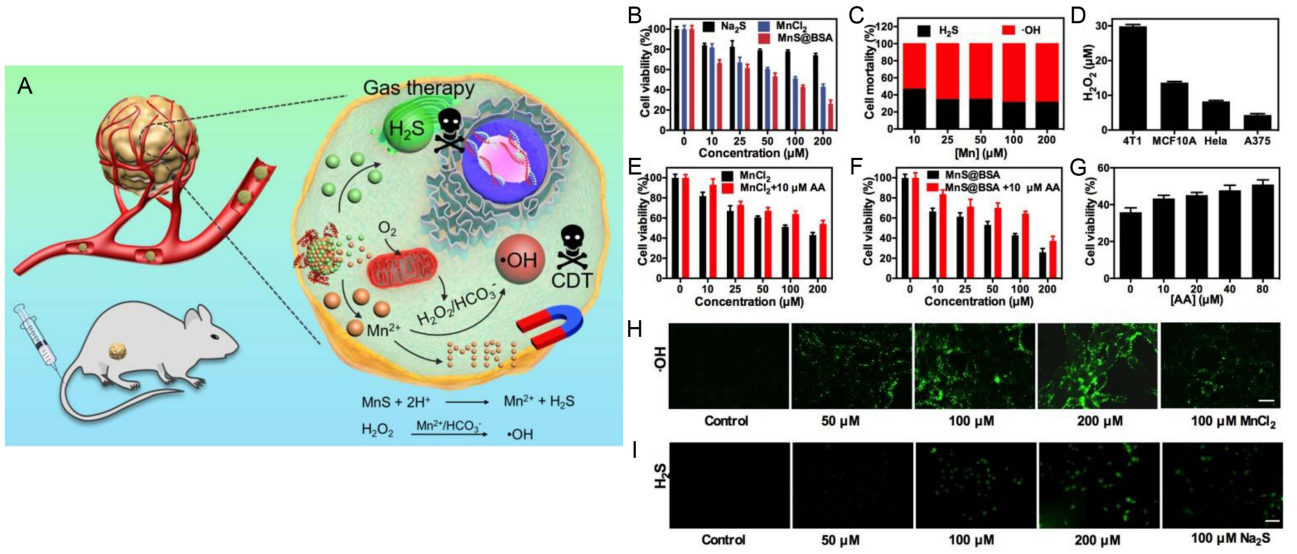

Figure 4 (**A**) MnS@BSA for tumor pH-responsive traceable hydrogen sulfide (H_2S) gas therapy primed CDT of cancer. The MnS@BSA can be degraded in response to the mildly acidic TME, releasing H_2S for gas therapy and Mn^{2+} for MRI and CDT of cancer. (**B**) Cell viability of 4T1 cells after incubation with Na_2S, $MnCl_2$ and MnS@BSA at different concentrations for 24 h. (**C**) Mortality of 4T1 cells caused by •OH radicals and H_2S gas after incubated with MnS@BSA for 24 h. (**D**) H_2O_2 concentrations in 4T1, MCF10A, HeLa, A375 cells detected by a H_2O_2 kit. Viability of 4T1 cells incubated with (**E**) $MnCl_2$, $MnCl_2$+10 μM L-ascorbic acid (AA) (**F**) MnS@BSA, MnS@BSA+10 μM AA. (**G**) Cytotoxicity of 4T1 cells incubated with 200 μM of MnS@BSA and various concentrations of AA: 0, 10, 20, 40, 80 μM for 24 h. (**H**) Confocal images of 4T1 cells incubated with various concentration of MnS@BSA: 0, 50, 100, 200 μM and $MnCl_2$: 100 μM for 4 h and stained with DCFH-DA fluorescence probe. (**I**) Fluorescence images of 4T1 cells incubated with WSP-5 H_2S fluorescence probe for 30 min, subsequently adding various concentration of MnS@BSA: 0, 50, 100, 200 μM and Na_2S 100 μM for 30 min, scale bar 100 μm. Reprinted from He T, Qin X, Jiang C, et al. Tumor pH-responsive metastable-phase manganese sulfide nanotheranostics for traceable hydrogen sulfide gas therapy primed chemodynamic therapy. Reprinted from He T, Qin X, Jiang C, et al. Tumor pH-responsive metastable-phase manganese sulfide nanotheranostics for traceable hydrogen sulfide gas therapy primed chemodynamic therapy. *Theranostics*. 2020;10(6):2453–2462, Creative Commons.[51]

efficiently kill osteosarcoma (Figure 5). Similarly, Tang et al[27] constructed Mn-doped silica NPs loaded with sorafenib using an optimized one-pot Stobers method, which fought tumor cells by disrupting intracellular redox homeostasis via GSH consumption. Furthermore, Keca et al[94] described a novel Mn-texaphyrin-phospholipid building block and its Mn-nanotexaphyrin assembly for the MRI-enhanced visualization of lymphatic drainage of proximal lymph nodes in the head and neck of VX-2 tumors. Jin et al[47] explored monolayer double-anchored Mn boride nanosheets as a novel metallic boride, MBene. The nanosystem exhibited unique NIR photothermal and photoacoustic effects, X-ray absorption, and MRI properties, having excellent potential in multimodal cancer imaging-induced PTT for cancer.

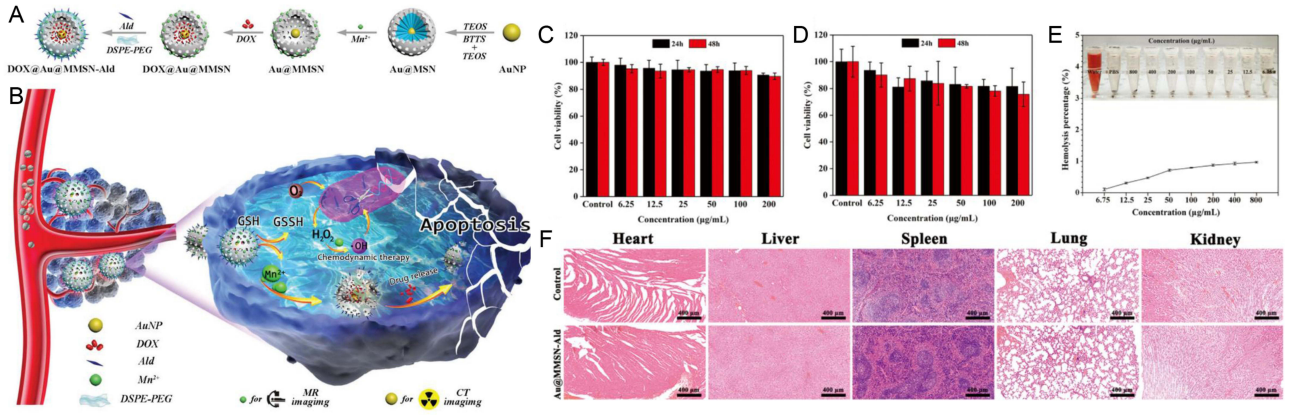

Figure 5 (**A**) Synthesis steps of DOX@Au@MMSN-Ald. (**B**) Upon targeted endocytosis, DOX@Au@MMSN-Ald treated by H_2O_2 and GSH can release Fenton-like initiator Mn^{2+} from the Mn–O–Si framework, which achieved CT/MR dual-modality imaging guided chemo-chemodynamic combination therapy. (**C**) Cell viability assay of (**C**) HUVECs and (**D**) RAW264.7 cells incubated with Au@MMSN-Ald suspensions at different concentrations for 24 h and 48 h. (**E**) Hemolytic percentage of RBCs after incubation with Au@MMSN-Ald suspensions. (**F**) H&E stained sections of major organs after 7 days of treatment for the control group and Au@MMSN-Ald group. Reprinted from Sha Z, Yang S, Fu L, et al. Manganese-doped gold core mesoporous silica particles as a nanoplatform for dual-modality imaging and chemo-chemodynamic combination osteosarcoma therapy. Reprinted from Sha Z, Yang S, Fu L, et al. Manganese-doped gold core mesoporous silica particles as a nanoplatform for dual-modality imaging and chemo-chemodynamic combination osteosarcoma therapy. *Nanoscale*. 2021;13(9):5077–5093, permission converyed through Copyright Clearance Center, Inc.[93]

Based on the above, multifunctional Mn-doped inorganic nonmetallic nanoreagents have been used as multimode imaging probes or effective therapeutics for remote detection and eradication of tumors. In addition, this kind of nanoreagents still have a lot of exploration space, and the subsequent generation of new nanomaterials is likely to be accompanied by noteworthy characteristics. Such nano-compounds will pave the way for other MRI-related cancer diagnosis and treatment.

Mn Ferrite

As a typical representative of Mn ferrite composites, $MnFe_2O_4$ NPs exhibit ideal magnetic targeting and remarkable NIR light responsiveness to promote their high tumor localization. Therefore, this magnetic nanosystem has great potential for simultaneous cancer diagnosis and accurate phototherapy. In a previous study, Kim et al[47] designed biocompatible Mn ferrite NPs and encapsulated them into mesoporous silica NPs to overcome hypoxia, thus improving in vivo PDT outcomes for cancer. After further modification, Deng et al[95] functionalized $MnFe_2O_4$ with an NIR dye, IR806, to obtain a nanosystem with excellent magnetic targeting and MRI capabilities. These functionalized nanomaterials concentrated specifically at the tumor site under an external magnetic field and 808 nm laser irradiation and completely destroyed subcutaneous solid tumors. To confirm this phenomenon, Ding et al[48] doped PEG-modified $MnFe_2O_4$ loaded with a photosensitizer into macroporous silica NPs. The nanocomposite achieved both magnetic targeting and the ability to overcome tumor hypoxia and was used for NIR-excitation and O_2 adaptive photodynamic cancer treatment.

In addition to inducing phototherapy, Yang et al[96] reported Mn ferrite nanocapsules as a delivery vehicle for acoustic sensitizer to release active cargoes at specific tumor sites and enhance the efficacy of sonodynamic therapy in cancer.

Based on monotherapy, MRI-guided multiple therapies derived from Mn ferrite nanostructures have also achieved considerably in research. For example, Rio et al[97] and Rodrigues et al[98] developed multifunctional liposomes loaded with gold-modified Mn-ferrite NPs for combined chemotherapy and phototherapy in cancer, respectively. Ribeiro et al[99] synthesized mixed magnetic liposomes of calcium-Mn ferrite by citrate co-precipitation and the sol-gel method, which were used for pH and temperature dual-sensitive chemotherapy and magnetic hyperthermia synergistic anticancer. In another ingenious design, He et al[100] prepared PEG-functionalized Mn ferrite NPs. The nanoplatform continuously catalyzed the decomposition of endogenous H_2O_2 to achieve oxygen self-sufficiency, while consuming GSH to reduce the loss of reactive oxygen species during radiotherapy, thus achieving an exciting combination of radiotherapy and CDT. Furthermore, Wang et al[101] prepared block copolymer micelles containing HA and Mn-Zn ferrite NPs using a two-step method, which significantly improved the efficiency of hyperthermia and radiotherapy against lung cancer. These findings confirm the great potential of Mn ferrite as an effective theranostic agent for cancer treatment.

In brief, Mn ferrite nanocomposites, such as $MnFe_2O_4$ or anisotropic Mn-Zn ferrite NPs, exhibit strong NIR light absorption, good photothermal stability, excellent MRI ability, and potential advantages in MRI-enhanced tumor observation and treatment evaluation. Table 4 described the applications of Mn ferrite in cancer diagnosis and treatment.

Mn Salt

A variety of Mn salt NPs, such as Mn silicate, Mn carbonate, Mn phosphate, and Mn phthalate, have the advantages of multi-responsive space-biological distribution and low systemic toxicity, which provide them with great clinical potential in time-dependent bioimaging-mediated cancer theranostics. For example, Nafiujjaman et al[102] developed a nanocomposite composed of hollow Mn silicate NPs and Ce6, which generated a large amount of oxygen under irradiation to alleviate tumor hypoxia and improve the effect of PDT against breast cancer. Liu et al[103] coated mesoporous copper/Mn silicate nanospheres with a biodegradable cancer cell membrane, showing good CDT/PDT synergistic efficacy against lung cancer. Furthermore, Xu et al[104] first proposed a tumor catalytic therapy strategy based on an immunomodulatory nanase to realize the synergistic regulation of nanases and TME. The nanase was composed of PEGylated iron Mn silicate NPs loaded with a transforming growth factor (TGF)-β inhibitor and showed effective anti-colorectal cancer activity. Wang et al[32] synthesized an iron inducer based on arginine-rich Mn silicate nanospheres using a one-pot reaction method, which demonstrated efficient GSH depletion capacity and T_1-weighted MRI-enhanced on-demand chemotherapeutic drug delivery behavior.

Table 4 Applications of Mn Ferrite Theranostics in Cancer Diagnosis and Treatment

Theranostics	Synthesis Method	Shape	Size (nm)	Therapeutic Mode	Therapeutic Cancer/Tumor	Ref.
Mn ferrite (MFMSNs)	Nucleophilic substitution reaction	Cubic spinel crystal structure	6	PDT	U-87 MG human brain astroglioblastoma cells	[47]
MFO-IR NPs	Thermal decomposition method	Spherical	16	PDT PTT	H22 mouse liver cancer cells	[95]
PEG-modified $MnFe_2O_4$ (UCMnFe-PS-PEG)	Hydrothermal method	Uniform, monodispersed and dendritic	3.5	PDT	HepG2 human liver cancer cells	[48]
Mn ferrite (ALA-hMVs)	Thermal decomposition	Vesicular structure	129.9 ± 16.3	Sonodynamic therapy	B16 mouse melanoma cells	[96]
Mn ferrite/Gold NPs	Co-precipitation	Spherical	26.7	Chemotherapy PTT	NCI-H460 human large cell lung cancer cells	[97]
Liposomes containing Mn ferrite/gold core/shell NPs	Co-precipitation	Spherical	152 ± 18	Chemotherapy PDT	A375-C5 human malignant melanoma cells and NCI-H460 human large cell lung cancer cells	[98]
Calcium-Mn ferrite magnetic NPs	Co-precipitation sol gel method	Spherical	8	Chemotherapy magnetic hyperthermia	HCT-15 human colorectal adenocarcinoma cells and NCI-H460 human large cell lung cancer cells	[99]
$MnFe_2O_4$-PEG	High-temperature reaction	Nanocube	15	Radiotherapy	4T1 mouse breast cancer cells	[100]
MZF-HA	High-temperature thermal decomposition method	Spherical	150	Hyperthermia radiotherapy	A549 human lung adenocarcinoma cells	[101]

Abbreviations: MFO, $MnFe_2O_4$; UC, upconversion; PS, photosensitizer; ALA, δ-aminolevulinic acid; hMVs, hypoxia-responsive nanovesicle; MZF, Mn-Zn ferrite; Ref, reference.

The excellent performance of Mn silicate NPs in imaging-guided antitumor activity has encouraged scientists to explore other Mn salt nanomaterials for biomedical applications. Xiao et al[105] prepared iron oxide NPs coated with nanoselenium, deposited it with Mn carbonate, and showed CDT/laser therapy combination-induced apoptosis of triple-negative breast cancer cells. Hou et al[106] constructed TME-sensitive nanohybrids by encapsulating DOX and phospholipids into amorphous porous Mn-phosphate NPs, which showed good antitumor activity and effectively improved the survival of tumor-bearing mice. Zhu et al[107] designed a protocell-like nanoreactor in which hydrophilic glucose oxidase was loaded into the pores of mesoporous silica NPs and hydrophobic Mn phthalate was loaded into the membrane layer of liposomes. The nanosystem synergistically enhanced the antitumor effects of PDT as starvation therapy for breast cancer (Figure 6).

Therefore, the construction and application of Mn-salt-based nanomaterials may provide new insights into targeted cancer therapy. However, there is still a need to improve the specificity, biocompatibility, and targeting efficiency of diagnostic CDT/PDT nano-agents.

At present, inorganic Mn contrast agents and their applications in cancer theranostics have been widely studied and developed. These exciting results are gradually known and recognized by peers in the field. However, it is necessary to further investigate their long-term stability, biodistribution and metabolic kinetics characteristics to promote the clinical transformation process of Mn-based MRI contrast agents. The solution of these problems is inseparable from the collaborative exploration of various disciplines including chemistry, biology and biomedical engineering.

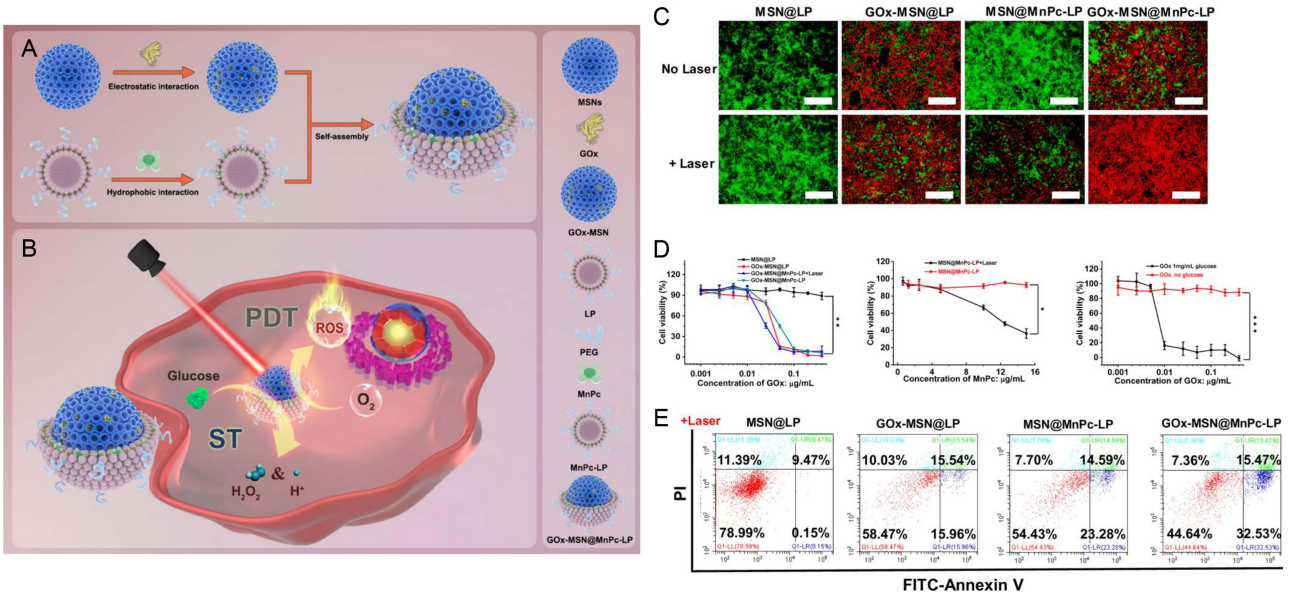

Figure 6 (**A**) Synthesis of a dual functional nanoreactor. (**B**) Consumption of glucose-controlled generation of reactive oxygen species upon laser irradiation for synergistic cancer treatment. (**C**) Fluorescence imaging of live/dead cells. 4T1 cells were treated with 200 μg/mL NPs and stained with 5 μM fluorescein diacetate (FDA) (green for live cells) and 10 μM propidium iodide (PI) (red for dead cells) (scale bar= 200 μm). (**D**) Cytotoxicity measurement by MTT assay. 4T1 cells were treated with different NPs, and the cells were analyzed by cytometry measurement. Error bars represent standard deviation from five measurements. (**E**) Annexin V/PI assay. Cells were treated with 200 μg/mL NPs at a concentration of 0.02 μg/mL GOx and 15 μg/mL MnPc (n = 3; *p < 0.05, **p < 0.01, ***p < 0.001 (*t*-test). Reprinted from Zhu Y, Shi H, Li T, et al. A dual functional nanoreactor for synergistic starvation and photodynamic therapy. Reprinted with permission from Zhu Y, Shi H, Li T, et al. A dual functional nanoreactor for synergistic starvation and photodynamic therapy. ACS Appl Mater Interfaces. 2020;12(16):18309–18318. Copyright © 2020 American Chemical Society.[107]

Organic Mn Contrast Agent-Mediated Cancer Theranostics

Metal-Organic Small Molecule Complex

Mn-based nanoMOFs are effective biomedical materials that can be easily synthesized and used for cancer detection and treatment. For example, Wang et al[108] designed a spindle copper (II) TCPP nanometal-organic skeleton (PCN-224(Cu)-GOD@MnO_2) to reduce the antioxidant activity of tumors and improve CDT efficacy. Zeng et al[109] prepared a hollow monodisperse MOF multifunctional nanoplatform containing Mn oxide NPs and FA, which has great potential as an intelligent cancer therapy. Furthermore, Wang et al[110] proposed an Mn MOF-derived multifunctional mesoporous nanase to generate endogenous O_2 in situ under the guidance of bioimaging and improved the efficacy of PDT (Figure 7). In addition, Bao et al[37] designed a nanoMOF based on a Hf cluster and a Mn (III)-porphyrin ligand, which showed significant tumor growth inhibition as a high-performance therapeutic agent.

In summary, Mn-based nanoMOFs have achieved excellent clinical and preclinical outcomes as adjuncts in TME-stimulated multimodal biomedical diagnosis and real-time treatment monitoring of cancer. However, the therapeutic effect of PDT is still limited by excitation light depth, high levels of GSH, and hypoxia in the TME.

Other Organic-Modified Mn

The high dynamic inertia and r_1 relaxation of organic-modified Mn nanocomplexes make them clinically approved as tumor-specific MRI contrast agents. For instance, Cao et al[111] synthesized a bimetallic complex containing Mn (II) and Cu (II) for CDT of lung cancer. Yang et al[112] modified photoresponsive NPs with aptamers (labeled Mn-D@BPFe-A) for lactic acid oxidation and cancer phototherapy. Mn-D@BPFe-A was constructed by assembling a functional complex with BSA followed by surface metal coordination to identify Fe^{3+} with a GAG sequence. Tabatabayi et al[113] synthesized the Mn (II) complex of N,N-bispyridoxine (1,4-butyleneamine) Schiff base, which showed effective pro-apoptotic and antioxidant activities against HepG2 and MCF7 cells, demonstrating its excellent potential for treating liver and breast cancers.

Mn-porphyrin compounds are another candidate for cancer diagnosis and treatment. Thamilarasan et al[114] demonstrated that redox-activated Mn porphyrins have significant effects on the treatment of vascular occlusion in humanized sickle mice with acute vascular occlusion crisis (Figure 8). Shrishrimal et al[115] found that tetraporphyrins and other Mn (III) porphyrins were effective radioprotectors that prevented radiation-induced fibrosis and activated the NRF2 signaling

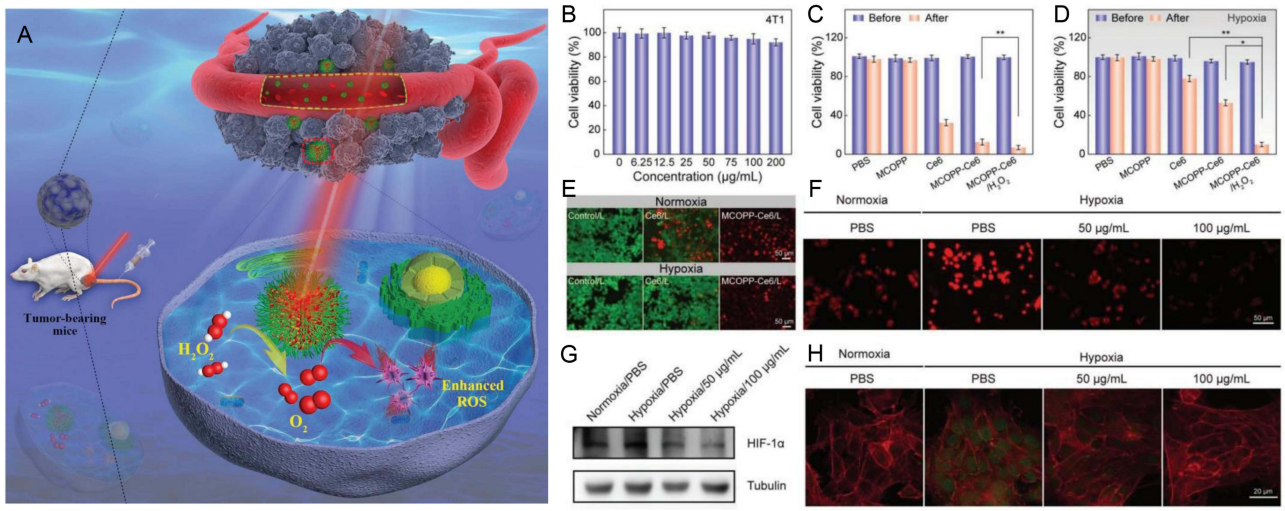

Figure 7 (**A**) Schematic illustration of MOF-derived mesoporous nanoenzyme (NE) for enhanced PDT of cancer. (**B**) Viability of 4T1 cells treated with MnCoO–PDA–PEG (MCOPP) NE at different concentrations. (**C and D**) Cell viability assay of 4T1 cells treated under different conditions in normoxic (**C**) and hypoxic (**D**) environments before and after 671 nm laser light irradiation. (**E**) Live/dead cell assay for cells treated with PBS, free Ce6 and MCOPP-Ce6 under normoxic and hypoxic conditions. (**F**) Confocal laser scanning microscopy (CLSM) images of 4T1 cells stained by O2 indicator, ie, $(Ru(dpp)_3)Cl_2$, after different treatments. (**G**) Western blots of HIF-1α expression in 4T1 cells treated with MCOPP NE. (**H**) CLSM images of HIF-1α (green) and F-actin (red) in cells incubated with MCOPP NE under normoxic and hypoxic conditions. Statistical analysis was performed using the Student's two-tailed *t*-test (*p < 0.05 and **p < 0.01). Reprinted with permission from Wang D, Wu H, Lim WQ, et al. A mesoporous nanoenzyme derived from metal-organic frameworks with endogenous oxygen generation to alleviate tumor hypoxia for significantly enhanced photodynamic therapy. *Adv Mater.* 2019;31(27):e1901893. Copyright © 2019 John Wiley and Sons.[110]

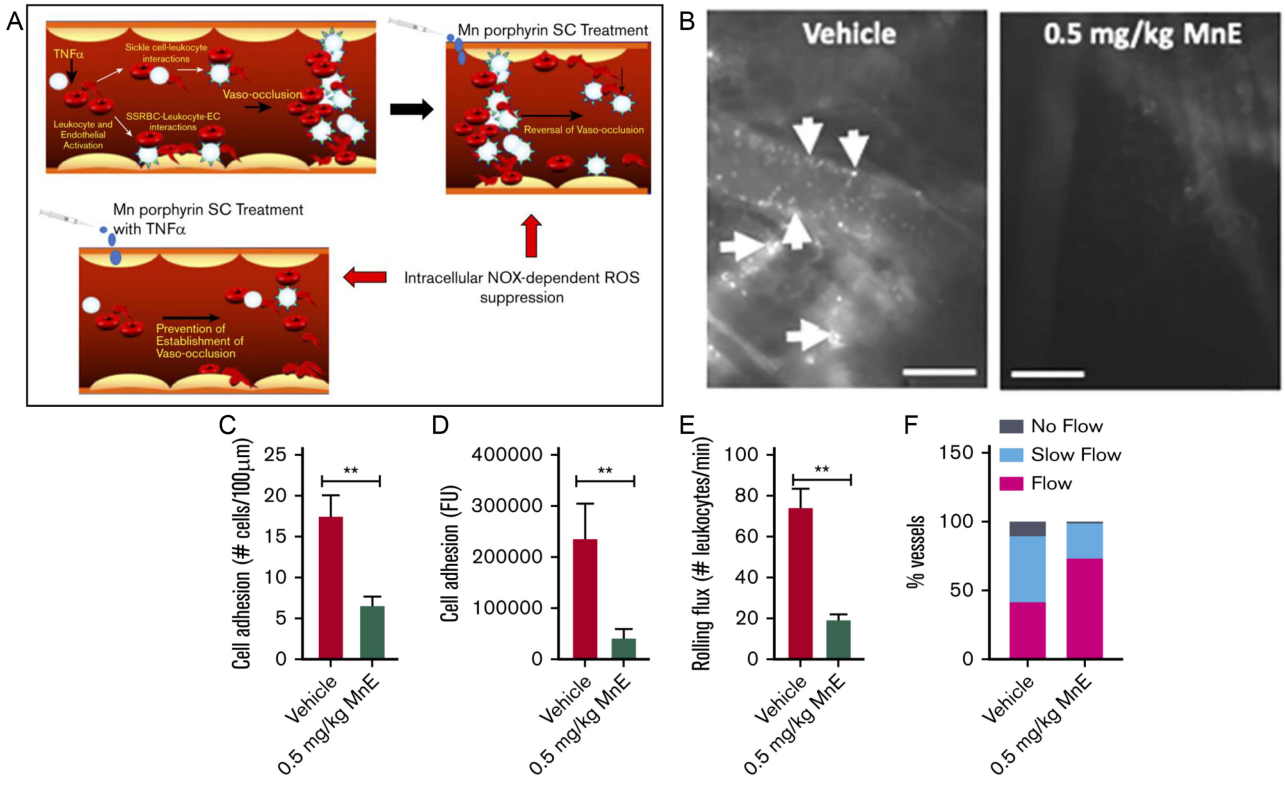

Figure 8 (**A**) Summarizes the Mn porphyrin sickle cell (SC) treatment with TNFα. (**B**) Intravital microscopy was performed on anesthetized treated TS mice. Representative images of postcapillary venules (20× magnification) from treated TS mice are presented. Leukocyte and RBC adhesion and vaso-occlusion are indicated with arrows. Scale bars, 50 μm. (**C-E**) Video frames showing vessel segments were used to quantify fluorescence-labeled cell (leukocyte and RBC) adhesion (**C** and **D**) and leukocyte rolling flux (**E**) in all venules and arterioles were recorded, and numbers were averaged among groups of animals. Cell adhesion presented as number of adherent cells per 100 μm vessel length (**C**), and fluorescence unit (FU) (**D**). Leukocyte rolling flux presented as number of leukocytes per minute (**E**). TS mice injected simultaneously with 1 dose of 0.5 mg/kg MnE and TNF-α showed sporadic cell adhesion (**C** and **D**) and reduced leukocyte rolling (**E**) as opposed to the vehicle group. (**F**) Blood flow in vivo. Percentage of vessels with normal, slow, and no blood flow (occluded vessels) are shown. Average vessel diameter was almost identical (~21 μm) in all treatment groups. Blood stasis in TS mice treated with 0.5 mg/kg MnE was significantly reduced compared with the vehicle group. Error bars show SEM of 6 different experiments for each treatment group. **P < 0.01 compared with vehicle treatment regardless of the vessel diameter within the ranges specified. Reprinted from Thamilarasan M, Estupinan R, Batinic-Haberle I, et al. Mn porphyrins as a novel treatment targeting sickle cell NOXs to reverse and prevent acute vaso-occlusion in vivo. *Blood Adv.* 2020;4(11):2372–2386. Permission conveyed through Copyright Clearance Center, Inc.[114]

pathway, partially explaining the mechanism of radiation protection in prostate fibroblasts. Furthermore, Chatterjee et al[116] demonstrated that Mn porphyrin, MnTE-2-PYP, significantly reduced prostate tumor size and improved survival. In addition, it lowered blood glucose levels and inhibited pro-fibrotic signaling in diabetic models.

Therefore, organic-functionalized Mn nanomaterials exhibit high drug loading, strong tumor targeting, good blood circulation stability, fast removal, low toxicity, and significant sensitivity in TME-responsive MRI-enhanced cancer treatment. However, synergistic CDT reduction of GSH levels with bimetallic complexes has not been reported, which is expected to improve the efficiency of CDT and promote clinical translation.

From the overall scale, the current research on organic Mn contrast agents is less than that of inorganic Mn, but this does not affect its important component as a Mn-based contrast agent. Inevitable technical barriers may be one of the factors leading to this result. Admittedly, this field needs to be further studied, but the excellent performance of the existing organic Mn contrast agents has attracted great interest from subsequent researchers.

Conclusion and Outlook

MRI is a rapidly developing molecular imaging technology owing to its non-invasiveness, high spatial and soft tissue resolution, non-ionizing radiation, and other qualities. In particular, the introduction of contrast agents alleviates the inherently low sensitivity of MRI, which has aroused widespread concern among researchers. Moreover, owing to their high relaxation efficiency, rapid water proton exchange rate, and good biocompatibility, various Mn-based nanomaterials have been developed as high-quality T_1 contrast agents, showing great clinical significance in cancer diagnosis and monitoring. In this review, the material properties, preparation strategies, and progress of Mn-related contrast agents in MRI-mediated cancer diagnosis and targeted therapy are discussed based on material classification.

However, there are still some challenges in translating Mn-contrast agent-associated nanomedicines into clinical practice. First, the limited understanding of the molecular mechanisms of tumorigenesis and development, especially immune networks in tumor progression, has largely hindered the application of Mn-based NPs in MRI-guided cancer therapy. Second, tumor heterogeneity and patient physical differences lead to individual variations in the therapeutic efficacy of the same nanodrug. Third, the toxicological mechanisms of NPs are not yet fully understood. Furthermore, given that the physicochemical properties of nanomedicines vary with the internal effects of biological substances, the ultimate dosage form must be carefully screened and evaluated. From a practical perspective, large-scale production of nanotheranostics of a uniform size, controllable morphology, and good reproducibility is difficult to transform from laboratory to commercial preparation.

Therefore, it is necessary to screen competitive tumor markers to guide the efficient enrichment and targeted delivery of NPs at specific sites in the body. Furthermore, the design of robust and repeatable experimental protocols is essential to comprehensively characterize and cross-verify the properties and functions of nanoprobe components in reasonable in vitro and in vivo models. In addition, the long-term toxicity, immunotoxicity, and neurotoxicity of NPs should be emphasized. With breakthroughs in interdisciplinary technology, these bottlenecks will be overcome smoothly, hence promoting the bright clinical prospect of Mn-based nanomaterials for precise cancer theranostics in the near future.

According to the characteristics and applications of Mn-based nanomaterials that have been reported at this stage, the future research trends should focus on the following five aspects. First of all, to enrich the current system by synthesizing of new Mn chelates agents, candidate nanotheranostics with different characteristics are of positive significance for the formulation of personalized solutions. Secondly, further improving the imaging contrast to enhance the resolution is always one of the key incentives for the research and development of this field. Thirdly, exploring solutions to achieve lower cytotoxicity and good biocompatibility is undoubtedly conducive to promoting the safe application of manganese-based nanomaterials. Subsequently, in-depth analysis of the mechanism of these nanomaterials is necessary for a broad understanding of their specific biological characteristics, but most of the current research is not sufficient in this regard. Last but not the least, to increase the clinical conversion rate of current research results, this may be initially improved through more representative animal models, such as patient derived xenograft model and humanized mice model, as well as extensive clinical trials in the later period.

Consent for Publication

All authors have read and approved the manuscript for submission.

Acknowledgments

This work was supported by the National Natural Science Foundation of China (81903662), the Scientific and Technological Innovation Programs of Higher Education Institutions in Shanxi (2019L0428), Basic Research Project of Shanxi Province (20210302124172), and the Startup Foundation for Doctors of Shanxi Medical University (XD1824).

Disclosure

The authors report no conflicts of interest in this work.

References

1. Siegel RL, Miller KD, Wagle NS, et al. Cancer statistics, 2023. *CA Cancer J Clin*. 2023;73(1):17–48. doi:10.3322/caac.21763
2. Wu C, Li M, Meng H, et al. Analysis of status and countermeasures of cancer incidence and mortality in China. *Sci China Life Sci*. 2019;62(5):640–647. doi:10.1007/s11427-018-9461-5
3. Cai X, Zhu Q, Zeng Y, et al. Manganese oxide nanoparticles as MRI contrast agents in tumor multimodal imaging and therapy. *Int J Nanomedicine*. 2019;14:8321–8344. doi:10.2147/IJN.S218085
4. Li Y, Cui J, Li C, et al. 19 F MRI nanotheranostics for cancer management: progress and prospects. *ChemMedChem*. 2022;17(4):e202100701. doi:10.1002/cmdc.202100701
5. Savla R, Garbuzenko OB, Chen S, et al. Tumor-targeted responsive nanoparticle-based systems for magnetic resonance imaging and therapy. *Pharm Res*. 2014;31(12):3487–3502. doi:10.1007/s11095-014-1436-x
6. Grover VP, Tognarelli JM, Crossey MM, et al. Magnetic resonance imaging: principles and techniques: lessons for clinicians. *J Clin Exp Hepatol*. 2015;5(3):246–255. doi:10.1016/j.jceh.2015.08.001
7. Li Y, Cheng Y, Zhang M, et al. A new compound with increased antitumor activity by cotargeting MEK and Pim-1. *iScience*. 2020;23(7):101254. doi:10.1016/j.isci.2020.101254
8. Li Y, Zhang C, Li G, et al. Protease-triggered bioresponsive drug delivery for the targeted theranostics of malignancy. *Acta Pharm Sin B*. 2021;11(8):2220–2242. doi:10.1016/j.apsb.2021.01.017
9. Li Y, Xin J, Sun Y, et al. Magnetic resonance imaging-guided and targeted theranostics of colorectal cancer. *Cancer Biol Med*. 2020;17(2):307–327. doi:10.20892/j.issn.2095-3941.2020.0072
10. Li Y, Zhang H. Nanoparticle-based drug delivery systems for enhanced tumor-targeting treatment. *J Biomed Nanotechnol*. 2019;15(1):1–27. doi:10.1166/jbn.2019.2670
11. Chowdhury M, Kras EA, Turowski SG, et al. Liposomal MRI probes containing encapsulated or amphiphilic Fe(iii) coordination complexes. *Biomater Sci*. 2023;11(17):5942–5954. doi:10.1039/d3bm00029j
12. Baranyai Z, Carniato F, Nucera A, et al. Defining the conditions for the development of the emerging class of Fe III -based MRI contrast agents. *Chem Sci*. 2021;12(33):11138–11145. doi:10.1039/d1sc02200h
13. Li Y, Mei T, Han S, et al. Cathepsin B-responsive nanodrug delivery systems for precise diagnosis and targeted therapy of malignant tumors. *Chin Chem Lett*. 2020;31(12):3027–3040. doi:10.1016/j.cclet.2020.05.027
14. An F, Yang Z, Zheng M, et al. Rationally assembled albumin/indocyanine green nanocomplex for enhanced tumor imaging to guide photothermal therapy. *J Nanobiotechnology*. 2020;18(1):49. doi:10.1186/s12951-020-00603-8
15. Li Y, Yang Y, An F, et al. Carrier-free, functionalized pure drug nanorods as a novel cancer-targeted drug delivery platform. *Nanotechnology*. 2013;24(1):15103. doi:10.1088/0957-4484/24/1/015103
16. Zhang J, An F, Li Y, et al. Simultaneous enhanced diagnosis and photodynamic therapy of photosensitizer-doped perylene nanoparticles via doping, fluorescence resonance energy transfer, and antenna effect. *Chem Commun (Camb)*. 2013;49(73):8072–8074. doi:10.1039/c3cc43413c
17. Li Y, Dong Q, Mei T, et al. Nanosized modification strategies for improving the antitumor efficacy of MEK inhibitors. *Curr Drug Targets*. 2020;21(3):228–251. doi:10.2174/1389450120666190807143245
18. Zhan Y, Shi S, Ehlerding EB, et al. Radiolabeled, antibody-conjugated manganese oxide nanoparticles for tumor vasculature targeted positron emission tomography and magnetic resonance imaging. *ACS Appl Mater Interfaces*. 2017;9(44):38304–38312. doi:10.1021/acsami.7b12216
19. Li Y, Zhang H. Fe(3)O(4)-based nanotheranostics for magnetic resonance imaging-synergized multifunctional cancer management. *Nanomedicine (Lond)*. 2019;14(11):1493–1512. doi:10.2217/nnm-2018-0346
20. An F, Li Y, Zhang J. Carrier-free photosensitizer nanocrystal for photodynamic therapy. *Mater Lett*. 2014;122:323–326. doi:10.1016/j.matlet.2014.02.067
21. Wu SC, Chen YJ, Wang HC, et al. Bispecific antibody conjugated manganese-based magnetic engineered iron oxide for imaging of HER2/neu- and EGFR-expressing tumors. *Theranostics*. 2016;6(1):118–130. doi:10.7150/thno.13069
22. Chang CC, Dinh TK, Lee YA, et al. Nanoparticle delivery of MnO(2) and antiangiogenic therapy to overcome hypoxia-driven tumor escape and suppress hepatocellular carcinoma. *ACS Appl Mater Interfaces*. 2020;12(40):44407–44419. doi:10.1021/acsami.0c08473
23. Zhu D, Zhu XH, Ren SZ, et al. Manganese dioxide (MnO 2) based nanomaterials for cancer therapies and theranostics. *J Drug Target*. 2021;29(9):911–924. doi:10.1080/1061186X.2020.1815209
24. Fu C, Duan X, Cao M, et al. Targeted magnetic resonance imaging and modulation of hypoxia with multifunctional hyaluronic acid-MnO(2) nanoparticles in glioma. *Adv Healthc Mater*. 2019;8(10):e1900047. doi:10.1002/adhm.201900047
25. Zhang C, Li L, Han FY, et al. Integrating fluorinated polymer and manganese-layered double hydroxide nanoparticles as pH-activated (19) F MRI agents for specific and sensitive detection of breast cancer. *Small*. 2019;15(36):e1902309. doi:10.1002/smll.201902309

26. Li M, Zhao Q, Yi X, et al. Au@MnS@ZnS Core/Shell/Shell nanoparticles for magnetic resonance imaging and enhanced cancer radiation therapy. *ACS Appl Mater Interfaces*. 2016;8(15):9557–9564. doi:10.1021/acsami.5b11588
27. Tang H, Li C, Zhang Y, et al. Targeted Manganese doped silica nano GSH-cleaner for treatment of Liver Cancer by destroying the intracellular redox homeostasis. *Theranostics*. 2020;10(21):9865–9887. doi:10.7150/thno.46771
28. Sterenczak KA, Meier M, Glage S, et al. Longitudinal MRI contrast enhanced monitoring of early tumour development with manganese chloride (MnCl2) and superparamagnetic iron oxide nanoparticles (SPIOs) in a CT1258 based in vivo model of prostate cancer. *BMC Cancer*. 2012;12:284. doi:10.1186/1471-2407-12-284
29. Zhang M, Cao Y, Wang L, et al. Manganese doped iron oxide theranostic nanoparticles for combined T1 magnetic resonance imaging and photothermal therapy. *ACS Appl Mater Interfaces*. 2015;7(8):4650–4658. doi:10.1021/am5080453
30. Xie J, Yan C, Yan Y, et al. Multi-modal Mn-Zn ferrite nanocrystals for magnetically-induced cancer targeted hyperthermia: a comparison of passive and active targeting effects. *Nanoscale*. 2016;8(38):16902–16915. doi:10.1039/c6nr03916b
31. Feng L, He F, Dai Y, et al. Multifunctional UCNPs@MnSiO(3)@g-C(3)N(4) nanoplatform: improved ROS generation and reduced glutathione levels for highly efficient photodynamic therapy. *Biomater Sci*. 2017;5(12):2456–2467. doi:10.1039/c7bm00798a
32. Wang S, Li F, Qiao R, et al. Arginine-rich manganese silicate nanobubbles as a ferroptosis-inducing agent for tumor-targeted theranostics. *ACS Nano*. 2018;12(12):12380–12392. doi:10.1021/acsnano.8b06399
33. Li XW, Zhao WR, Liu YJ, et al. Facile synthesis of manganese silicate nanoparticles for pH/GSH-responsive T-1-weighted magnetic resonance imaging. *J Mater Chem B*. 2016;4(24):4313–4321. doi:10.1039/c6tb00718j
34. Li X, Zhou H, Niu Z, et al. In Situ 3D-to-2D transformation of manganese-based layered silicates for tumor-specific T-1-weighted magnetic resonance imaging with high signal-to-noise and excretability. *ACS Appl Mater Interfaces*. 2020;12(22):24644–24654. doi:10.1021/acsami.0c07018
35. Shao C, Li S, Gu W, et al. Multifunctional gadolinium-doped manganese carbonate nanoparticles for targeted MR/fluorescence imaging of tiny brain gliomas. *Anal Chem*. 2015;87(12):6251–6257. doi:10.1021/acs.analchem.5b01639
36. Hao Y, Zheng C, Wang L, et al. Tumor acidity-activatable manganese phosphate nanoplatform for amplification of photodynamic cancer therapy and magnetic resonance imaging. *Acta Biomater*. 2017;62:293–305. doi:10.1016/j.actbio.2017.08.028
37. Bao J, Zu X, Wang X, et al. Multifunctional Hf/Mn-TCPP metal-organic framework nanoparticles for triple-modality imaging-guided PTT/RT synergistic cancer therapy. *Int J Nanomedicine*. 2020;15:7687–7702. doi:10.2147/IJN.S267321
38. Zheng S, Zhang M, Bai H, et al. Preparation of AS1411 Aptamer Modified Mn-MoS(2) QDs for Targeted MR imaging and fluorescence labelling of renal cell carcinoma. *Int J Nanomedicine*. 2019;14:9513–9524. doi:10.2147/IJN.S215883
39. Islam MK, Kim S, Kim HK, et al. Manganese complex of ethylenediaminetetraacetic Acid (EDTA)-Benzothiazole Aniline (BTA) Conjugate as a potential liver-targeting MRI contrast agent. *J Med Chem*. 2017;60(7):2993–3001. doi:10.1021/acs.jmedchem.6b01799
40. Islam MK, Kim S, Kim HK, et al. Synthesis and evaluation of manganese(II)-based ethylenediaminetetraacetic acid-ethoxybenzyl conjugate as a highly stable hepatobiliary magnetic resonance imaging contrast agent. *Bioconjug Chem*. 2018;29(11):3614–3625. doi:10.1021/acs.bioconjchem.8b00560
41. Ren Y, Sedgwick AC, Chen J, et al. Manganese(II) texaphyrin: a paramagnetic photoacoustic contrast agent activated by near-IR Light. *J Am Chem Soc*. 2020;142(38):16156–16160. doi:10.1021/jacs.0c04387
42. Foroushani MS, Niroumand N, Shervedani RK, et al. A theranostic system based on nanocomposites of manganese oxide nanoparticles and a pH sensitive polymer: preparation, and physicochemical characterization. *Bioelectrochemistry*. 2019;126:130. doi:10.1016/j.bioelechem.2019.107347
43. Peng C, Xing H, Xue Y, et al. Ratiometric sensing of alkaline phosphatase based on the catalytical activity from Mn-Fe layered double hydroxide nanosheets. *Nanoscale*. 2020;12(3):2022–2027. doi:10.1039/c9nr08769a
44. Li B, Gu Z, Kurniawan N, et al. Manganese-BASED LAYERED DOUBLE HYDROXIDE NAnoparticles as a T(1) -MRI contrast agent with ultrasensitive pH response and high relaxivity. *Adv Mater*. 2017;29(29). doi:10.1002/adma.201700373
45. Zuo H, Chen W, Li B, et al. MnAl layered double hydroxide nanoparticles as a dual-functional platform for magnetic resonance imaging and siRNA delivery. *Chemistry*. 2017;23(57):14299–14306. doi:10.1002/chem.201702835
46. Chen W, Wang X, Zhao B, et al. CuS-MnS(2) nano-flowers for magnetic resonance imaging guided photothermal/photodynamic therapy of ovarian cancer through necroptosis. *Nanoscale*. 2019;11(27):12983–12989. doi:10.1039/c9nr03114f
47. Kim J, Cho HR, Jeon H, et al. Continuous O(2)-Evolving MnFe(2)O(4) nanoparticle-anchored mesoporous silica nanoparticles for efficient photodynamic therapy in hypoxic cancer. *J Am Chem Soc*. 2017;139(32):10992–10995. doi:10.1021/jacs.7b05559
48. Ding B, Shao S, Xiao H, et al. MnFe(2)O(4)-decorated large-pore mesoporous silica-coated upconversion nanoparticles for near-infrared light-induced and O(2) self-sufficient photodynamic therapy. *Nanoscale*. 2019;11(31):14654–14667. doi:10.1039/c9nr04858h
49. Carniato F, Ricci M, Tei L, et al. Novel nanogels loaded with Mn(II) chelates as effective and biologically stable MRI Probes. *Small*. 2023:e2302868. doi:10.1002/smll.202302868
50. Yang R, Hou M, Gao Y, et al. Biomineralization-inspired crystallization of manganese oxide on silk fibroin nanoparticles for in vivo MR/fluorescence imaging-assisted tri-modal therapy of cancer. *Theranostics*. 2019;9(21):6314–6333. doi:10.7150/thno.36252
51. He T, Qin X, Jiang C, et al. Tumor pH-responsive metastable-phase manganese sulfide nanotheranostics for traceable hydrogen sulfide gas therapy primed chemodynamic therapy. *Theranostics*. 2020;10(6):2453–2462. doi:10.7150/thno.42981
52. Chen J, Zhang WJ, Guo Z, et al. pH-responsive iron manganese silicate nanoparticles as T1-T2* dual-modal imaging probes for tumor diagnosis. *ACS Appl Mater Interfaces*. 2015;7(9):5373–5383. doi:10.1021/acsami.5b00727
53. Pernia LM, Rivera-Fernandez S, Franco JM, et al. Long-circulating PEGylated manganese ferrite nanoparticles for MRI-based molecular imaging. *Nanoscale*. 2015;7(5):2050–2059. doi:10.1039/c4nr05781c
54. Miao ZH, Wang H, Yang H, et al. Intrinsically Mn 2+ -chelated polydopamine nanoparticles for simultaneous magnetic resonance imaging and photothermal ablation of cancer cells. *ACS Appl Mater Interfaces*. 2015;7(31):16946–16952. doi:10.1021/acsami.5b06265
55. Sonis ST. Superoxide dismutase as an intervention for radiation therapy-associated toxicities: review and profile of avasopasem manganese as a treatment option for radiation-induced mucositis. *Drug Des Devel Ther*. 2021;15:1021–1029. doi:10.2147/DDDT.S267400
56. Cheng J, Zhu Y, Xing X, et al. Manganese-deposited iron oxide promotes tumor-responsive ferroptosis that synergizes the apoptosis of cisplatin. *Theranostics*. 2021;11(11):5418–5429. doi:10.7150/thno.53346

57. Zou R, Li J, Yang T, et al. Biodegradable manganese engineered nanocapsules for tumor-sensitive near-infrared persistent luminescence/magnetic resonance imaging and simultaneous chemotherapy. *Theranostics*. 2021;11(17):8448–8463. doi:10.7150/thno.59840
58. Wu Y, Huang Y, Tu C, et al. A mesoporous polydopamine nanoparticle enables highly efficient manganese encapsulation for enhanced MRI-guided photothermal therapy. *Nanoscale*. 2021;13(13):6439–6446. doi:10.1039/d1nr00957e
59. Sishc BJ, Ding L, Nam TK, et al. Avasopasem manganese synergizes with hypofractionated radiation to ablate tumors through the generation of hydrogen peroxide. *Sci Transl Med*. 2021;13(593). doi:10.1126/scitranslmed.abb3768
60. Yi M, Niu M, Zhang J, et al. Combine and conquer: manganese synergizing anti-TGF-beta/PD-L1 bispecific antibody YM101 to overcome immunotherapy resistance in non-inflamed cancers. *J Hematol Oncol*. 2021;14(1):146. doi:10.1186/s13045-021-01155-6
61. Lv M, Chen M, Zhang R, et al. Manganese is critical for antitumor immune responses via cGAS-STING and improves the efficacy of clinical immunotherapy. *Cell Res*. 2020;30(11):966–979. doi:10.1038/s41422-020-00395-4
62. Xiao J, Yan M, Zhou K, et al. A nanoselenium-coating biomimetic cytomembrane nanoplatform for mitochondrial targeted chemotherapy- and chemodynamic therapy through manganese and doxorubicin codelivery. *J Nanobiotechnology*. 2021;19(1):227. doi:10.1186/s12951-021-00971-9
63. Zhu D, Liu Z, Li Y, et al. Delivery of manganese carbonyl to the tumor microenvironment using Tumor-Derived exosomes for cancer gas therapy and low dose radiotherapy. *Biomaterials*. 2021;274:120894. doi:10.1016/j.biomaterials.2021.120894
64. Xu X, Zhang R, Yang X, et al. A honeycomb-like bismuth/manganese oxide nanoparticle with mutual reinforcement of internal and external response for triple-negative breast cancer targeted therapy. *Adv Healthc Mater*. 2021;10(18):e2100518. doi:10.1002/adhm.202100518
65. Zhu Y, Deng M, Xu N, et al. A tumor microenvironment responsive nanotheranostics agent for magnetic resonance imaging and synergistic photodynamic therapy/photothermal therapy of liver cancer. *Front Chem*. 2021;9:650899. doi:10.3389/fchem.2021.650899
66. Liu J, Qing X, Zhang Q, et al. Oxygen-producing proenzyme hydrogels for photodynamic-mediated metastasis-inhibiting combinational therapy. *J Mater Chem B*. 2021;9(26):5255–5263. doi:10.1039/d1tb01009c
67. Tan J, Duan X, Zhang F, et al. Theranostic nanomedicine for synergistic chemodynamic therapy and chemotherapy of orthotopic glioma. *Adv Sci (Weinh)*. 2020;7(24):2003036. doi:10.1002/advs.202003036
68. Wang H, Jia D, Yuan D, et al. Dimeric Her2-specific affibody mediated cisplatin-loaded nanoparticles for tumor enhanced chemo-radiotherapy. *J Nanobiotechnology*. 2021;19(1):138. doi:10.1186/s12951-021-00885-6
69. Luo M, Lv Y, Luo X, et al. Developing smart nanoparticles responsive to the tumor micro-environment for enhanced synergism of thermo-chemotherapy with PA/MR bimodal imaging. *Front Bioeng Biotechnol*. 2022;10:799610. doi:10.3389/fbioe.2022.799610
70. Zhang Y, Wang H, Jia X, et al. Cascade catalytic nanoplatform for enhanced starvation and sonodynamic therapy. *J Drug Target*. 2020;28(2):195–203. doi:10.1080/1061186X.2019.1641507
71. R A, Yao Y, Guo X, et al. Precise cancer anti-acid therapy monitoring using pH-Sensitive MnO(2)@BSA nanoparticles by magnetic resonance imaging. *ACS Appl Mater Interfaces*. 2021;13(16):18604–18618. doi:10.1021/acsami.1c04310
72. Hu Q, Zhang S, Zhu J, et al. The promotional effect of hollow MnO(2) with brucea javanica oil emulsion (BJOE) on endometrial cancer apoptosis. *Biomed Res Int*. 2021;2021:6631533. doi:10.1155/2021/6631533
73. Hou M, Liu W, Zhang L, et al. Responsive agarose hydrogel incorporated with natural humic acid and MnO(2) nanoparticles for effective relief of tumor hypoxia and enhanced photo-induced tumor therapy. *Biomater Sci*. 2020;8(1):353–369. doi:10.1039/c9bm01472a
74. Shen Z, Xia J, Ma Q, et al. Tumor Microenvironment-triggered Nanosystems as dual-relief Tumor Hypoxia Immunomodulators for enhanced Phototherapy. *Theranostics*. 2020;10(20):9132–9152. doi:10.7150/thno.46076
75. Shi M, Wang S, Zheng S, et al. Activatable MRI-monitoring gene delivery for the theranostic of renal carcinoma. *Colloids Surf B Biointerfaces*. 2020;185:110625. doi:10.1016/j.colsurfb.2019.110625
76. Nie Y, Li D, Peng Y, et al. Metal organic framework coated MnO(2) nanosheets delivering doxorubicin and self-activated DNAzyme for chemo-gene combinatorial treatment of cancer. *Int J Pharm*. 2020;585:119513. doi:10.1016/j.ijpharm.2020.119513
77. Wang H, An L, Tao C, et al. A smart theranostic platform for photoacoustic and magnetic resonance dual-imaging-guided photothermal-enhanced chemodynamic therapy. *Nanoscale*. 2020;12(8):5139–5150. doi:10.1039/c9nr10039c
78. Fan S, Zhang Y, Tan H, et al. Manganese/iron-based nanoprobes for photodynamic/chemotherapy combination therapy of tumor guided by multimodal imaging. *Nanoscale*. 2021;13(10):5383–5399. doi:10.1039/d0nr08831e
79. Jain P, Bhagat S, Tunki L, et al. Serotonin-stearic acid bioconjugate-coated completely biodegradable Mn(3)O(4) nanocuboids for hepatocellular carcinoma targeting. *ACS Appl Mater Interfaces*. 2020;12(9):10170–10182. doi:10.1021/acsami.0c00331
80. Ding D, Feng Y, Qin R, et al. Mn(3+)-rich oxide/persistent luminescence nanoparticles achieve light-free generation of singlet oxygen and hydroxyl radicals for responsive imaging and tumor treatment. *Theranostics*. 2021;11(15):7439–7449. doi:10.7150/thno.62437
81. Guan S, Liu X, Li C, et al. Intracellular mutual amplification of oxidative stress and inhibition multidrug resistance for enhanced sonodynamic/chemodynamic/chemo therapy. *Small*. 2022;18(13):e2107160. doi:10.1002/smll.202107160
82. Liu Q, Shi L, Liao Y, et al. Ultrathin-FeOOH-Coated MnO(2) sonosensitizers with boosted reactive oxygen species yield and remodeled tumor microenvironment for efficient cancer therapy. *Adv Sci (Weinh)*. 2022;9(17):e2200005. doi:10.1002/advs.202200005
83. Tang S, Zhou L, He H, et al. MnO(2)-melittin nanoparticles serve as an effective anti-tumor immunotherapy by enhancing systemic immune response. *Biomaterials*. 2022;288:121706. doi:10.1016/j.biomaterials.2022.121706
84. Deng Z, Xi M, Zhang C, et al. Biomineralized MnO(2) nanoplatforms mediated delivery of immune checkpoint inhibitors with STING pathway activation to potentiate cancer radio-immunotherapy. *ACS Nano*. 2023;17(5):4495–4506. doi:10.1021/acsnano.2c10352
85. Wang X, Ding C, Zhang Z, et al. Degradable nanocatalyst enables antitumor/antibacterial therapy and promotion of wound healing for diabetes via self-enhanced cascading reaction. *Chin Chem Lett*. 2023;34(7):107951. doi:10.1016/j.cclet.2022.107951
86. Xie W, Guo Z, Gao Q, et al. Manganese-doped layered double hydroxide: a biodegradable theranostic nanoplatform with tumor microenvironment response for magnetic resonance imaging-guided photothermal therapy. *ACS Appl Bio Mater*. 2020;3(9):5845–5855. doi:10.1021/acsabm.0c00564
87. Wen J, Lv Y, Xu Y, et al. Construction of a biodegradable, versatile nanocarrier for optional combination cancer therapy. *Acta Biomater*. 2019;83:359–371. doi:10.1016/j.actbio.2018.11.009
88. Liao L, Cen D, Fu Y, et al. Biodegradable MnFe-hydroxide nanocapsules to enable multi-therapeutics delivery and hypoxia-modulated tumor treatment. *J Mater Chem B*. 2020;8(17):3929–3938. doi:10.1039/d0tb00243g

89. Yan L, Wang Y, Hu T, et al. Layered double hydroxide nanosheets: towards ultrasensitive tumor microenvironment responsive synergistic therapy. *J Mater Chem B*. 2020;8(7):1445–1455. doi:10.1039/c9tb02591j
90. Ke K, Yang W, Xie X, et al. Copper manganese sulfide nanoplates: a new two-dimensional theranostic nanoplatform for MRI/MSOT dual-modal imaging-guided photothermal therapy in the second near-infrared window. *Theranostics*. 2017;7(19):4763–4776. doi:10.7150/thno.21694
91. Irmania N, Dehvari K, Gedda G, et al. Manganese-doped green tea-derived carbon quantum dots as a targeted dual imaging and photodynamic therapy platform. *J Biomed Mater Res B Appl Biomater*. 2020;108(4):1616–1625. doi:10.1002/jbm.b.34508
92. Atif M, Iqbal S, Fakhar-E-Alam M, et al. Manganese-doped cerium oxide nanocomposite as a therapeutic agent for MCF-7 adenocarcinoma cell line. *Saudi J Biol Sci*. 2021;28(2):1233–1238. doi:10.1016/j.sjbs.2020.12.006
93. Sha Z, Yang S, Fu L, et al. Manganese-doped gold core mesoporous silica particles as a nanoplatform for dual-modality imaging and chemo-chemodynamic combination osteosarcoma therapy. *Nanoscale*. 2021;13(9):5077–5093. doi:10.1039/d0nr09220g
94. Keca JM, Chen J, Overchuk M, et al. Nanotexaphyrin: one-pot synthesis of a manganese texaphyrin-phospholipid nanoparticle for magnetic resonance imaging. *Angew Chem Int Ed Engl*. 2016;55(21):6187–6191. doi:10.1002/anie.201600234
95. Deng K, Chen Y, Li C, et al. 808 nm light responsive nanotheranostic agents based on near-infrared dye functionalized manganese ferrite for magnetic-targeted and imaging-guided photodynamic/photothermal therapy. *J Mater Chem B*. 2017;5(9):1803–1814. doi:10.1039/c6tb03233h
96. Yang K, Yue L, Yu G, et al. A hypoxia responsive nanoassembly for tumor specific oxygenation and enhanced sonodynamic therapy. *Biomaterials*. 2021;275:120822. doi:10.1016/j.biomaterials.2021.120822
97. Rio I, Rodrigues A, Rodrigues JM, et al. Magnetoliposomes based on magnetic/plasmonic nanoparticles loaded with tricyclic lactones for combined cancer therapy. *Pharmaceutics*. 2021;13(11):1905. doi:10.3390/pharmaceutics13111905
98. Rodrigues A, Matos J, Nova DA, et al. Development of multifunctional liposomes containing magnetic/plasmonic MnFe(2)O(4)/Au core/shell nanoparticles. *Pharmaceutics*. 2018;11(1):10. doi:10.3390/pharmaceutics11010010
99. Ribeiro BC, Alvarez C, Alves BC, et al. Development of Thermo- and pH-sensitive liposomal magnetic carriers for new potential antitumor thienopyridine derivatives. *Materials (Basel)*. 2022;15(5):1737. doi:10.3390/ma15051737
100. He Z, Yan H, Zeng W, et al. Tumor microenvironment-responsive multifunctional nanoplatform based on MnFe 2O 4 -PEG for enhanced magnetic resonance imaging-guided hypoxic cancer radiotherapy. *J Mater Chem B*. 2021;9(6):1625–1637. doi:10.1039/d0tb02631j
101. Wang Y, Zou L, Qiang Z, et al. Enhancing targeted cancer treatment by combining hyperthermia and radiotherapy using Mn-Zn ferrite magnetic nanoparticles. *ACS Biomater Sci Eng*. 2020;6(6):3550–3562. doi:10.1021/acsbiomaterials.0c00287
102. Nafiujjaman M, Chung SJ, Kalashnikova I, et al. Biodegradable hollow manganese silicate nanocomposites to alleviate tumor hypoxia toward enhanced photodynamic therapy. *ACS Appl Bio Mater*. 2020;3(11):7989–7999. doi:10.1021/acsabm.0c01079
103. Liu C, Wang D, Zhang S, et al. Biodegradable biomimic copper/manganese silicate nanospheres for chemodynamic/photodynamic synergistic therapy with simultaneous glutathione depletion and hypoxia relief. *ACS Nano*. 2019;13(4):4267–4277. doi:10.1021/acsnano.8b09387
104. Xu B, Cui Y, Wang W, et al. Immunomodulation-enhanced nanozyme-based tumor catalytic therapy. *Adv Mater*. 2020;32(33):e2003563. doi:10.1002/adma.202003563
105. Xiao J, Zhang G, Xu R, et al. A pH-responsive platform combining chemodynamic therapy with limotherapy for simultaneous bioimaging and synergistic cancer therapy. *Biomaterials*. 2019;216:119254. doi:10.1016/j.biomaterials.2019.119254
106. Hou L, Tian C, Yan Y, et al. Manganese-based nanoactivator optimizes cancer immunotherapy via enhancing innate immunity. *ACS Nano*. 2020;14(4):3927–3940. doi:10.1021/acsnano.9b06111
107. Zhu Y, Shi H, Li T, et al. A dual functional nanoreactor for synergistic starvation and photodynamic therapy. *ACS Appl Mater Interfaces*. 2020;12(16):18309–18318. doi:10.1021/acsami.0c01039
108. Wang Z, Liu B, Sun Q, et al. Fusiform-like copper(ii)-based metal-organic framework through relief hypoxia and GSH-Depletion Co-enhanced starvation and chemodynamic synergetic cancer therapy. *ACS Appl Mater Interfaces*. 2020;12(15):17254–17267. doi:10.1021/acsami.0c01539
109. Zeng X, Chen B, Song Y, et al. Fabrication of versatile hollow metal-organic framework nanoplatforms for folate-targeted and combined cancer imaging and therapy. *ACS Appl Bio Mater*. 2021;4(8):6417–6429. doi:10.1021/acsabm.1c00603
110. Wang D, Wu H, Lim WQ, et al. A mesoporous nanoenzyme derived from metal-organic frameworks with endogenous oxygen generation to alleviate tumor hypoxia for significantly enhanced photodynamic therapy. *Adv Mater*. 2019;31(27):e1901893. doi:10.1002/adma.201901893
111. Cao S, Fan J, Sun W, et al. A novel Mn-Cu bimetallic complex for enhanced chemodynamic therapy with simultaneous glutathione depletion. *Chem Commun (Camb)*. 2019;55(86):12956–12959. doi:10.1039/c9cc06040e
112. Yang H, Lu WL, Huang T, et al. An aptamer-Fe(3+) modified nanoparticle for lactate oxidation and tumor photodynamic therapy. *Colloids Surf B Biointerfaces*. 2018;164:192–200. doi:10.1016/j.colsurfb.2018.01.045
113. Tabatabayi ZS, Homayouni-Tabrizi M, Neamati A, et al. Mn(II) complex of a vitamin B6 Schiff base as an exclusive apoptosis inducer in human MCF7 and HepG2 cancer cells: synthesis, characterization, and biological studies. *J Cell Biochem*. 2020;121(3):2677–2689. doi:10.1002/jcb.29488
114. Thamilarasan M, Estupinan R, Batinic-Haberle I, et al. Mn porphyrins as a novel treatment targeting sickle cell NOXs to reverse and prevent acute vaso-occlusion in vivo. *Blood Adv*. 2020;4(11):2372–2386. doi:10.1182/bloodadvances.2020001642
115. Shrishrimal S, Chatterjee A, Kosmacek EA, et al. Manganese porphyrin, MnTE-2-PyP, treatment protects the prostate from radiation-induced fibrosis (RIF) by activating the NRF2 signaling pathway and enhancing SOD2 and sirtuin activity. *Free Radic Biol Med*. 2020;152:255–270. doi:10.1016/j.freeradbiomed.2020.03.014
116. Chatterjee A, Kosmacek EA, Shrishrimal S, et al. MnTE-2-PyP, a manganese porphyrin, reduces cytotoxicity caused by irradiation in a diabetic environment through the induction of endogenous antioxidant defenses. *Redox Biol*. 2020:34. doi:10.1016/j.redox.2020.101542